RUB

Evgeny Epelbaum, Ruhr University Bochum

CLUSHIQ2022, Sendai International Center, Japan, October 31 - November 3, 2022

Few-nucleon systems in chiral EFT: Recent developments

Introduction

Two-nucleons in χEFT

Few-nucleon systems at N^{2}LO

Precision calculation of charge radii of light nuclei

Towards solution of the 3NF challenge

Summary and outlook

Clusters & Hierarchies

Bundesministerium für Bildung und Forschung
DFG Deutsche Forschungsgemeinschaft
erc European Research Council

Chiral Effective Field Theory

GB dynamics
Weinberg, Gasser, Leutwyler, …

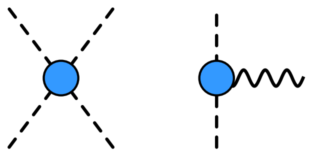

πN dynamics
Bernard-Kaiser-Meißner et al.

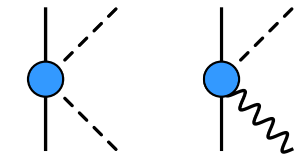

Chiral Perturbation Theory

$$Q = \frac{\text{momenta of particles or } M_\pi}{\text{breakdown scale } \Lambda_b} \sim \frac{1}{4} \cdots \frac{1}{3}$$

Effective Lagrangian:

$$\mathcal{L}_\pi = \frac{F^2}{4}\mathrm{Tr}(\nabla^\mu U \nabla_\mu U^\dagger + \chi_+) + \ldots ,$$

$$\mathcal{L}_{\pi N} = \bar{N}(iv\cdot D + g_A\, u\cdot S)N + \ldots ,$$

$$\mathcal{L}_{NN} = -\frac{1}{2}C_S(\bar{N}N)^2 + 2C_T(\bar{N}SN)^2 + \ldots$$

Nuclear forces
Weinberg, van Kolck, Kaiser, EGM, …

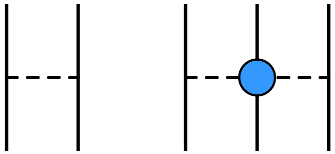

Nuclear currents
Park et al, Bochum-Bonn, JLab-Pisa

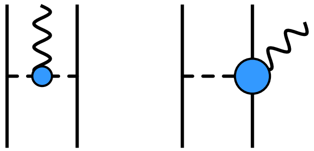

Combined with ab-initio few-body methods, provide first-principle approach to nuclear systems

Goal: chiral EFT as a precision tool

Chiral expansion of the nuclear forces [NDA, DimReg]

	Two-nucleon force	Three-nucleon force	Four-nucleon force
LO (Q^0)	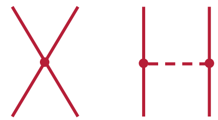 Weinberg '90	—	—
NLO (Q^2)	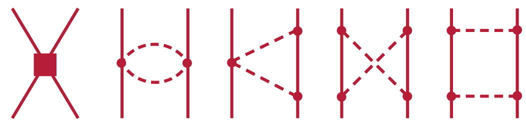 Ordonez, van Kolck '92	—	—
N²LO (Q^3)	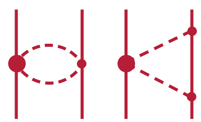 Ordonez, van Kolck '92	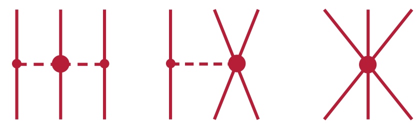 van Kolck '94; EE et al. '02	—
N³LO (Q^4)	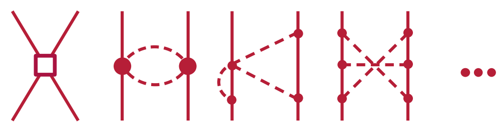 Kaiser '00 - '02	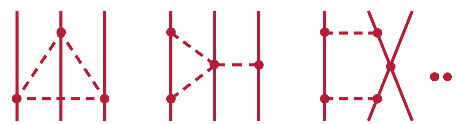 Bernard, EE, Krebs, Meißner,'08, '11	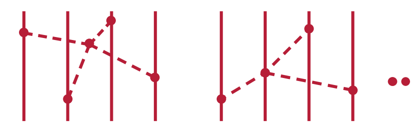 EE '06
N⁴LO (Q^5)	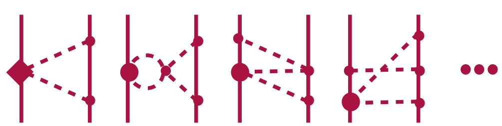 Entem, Kaiser, Machleidt, Nosyk '15 EE, Krebs, Meißner '15	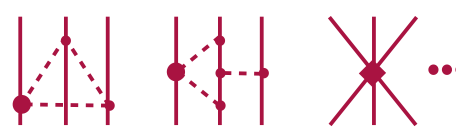 Girlanda, Kievsky, Viviani '11 Krebs, Gasparyan, EE '12,'13 (short-range loop contrib. still missing)	— (preliminary)

Chiral expansion of the nuclear forces [NDA, DimReg]

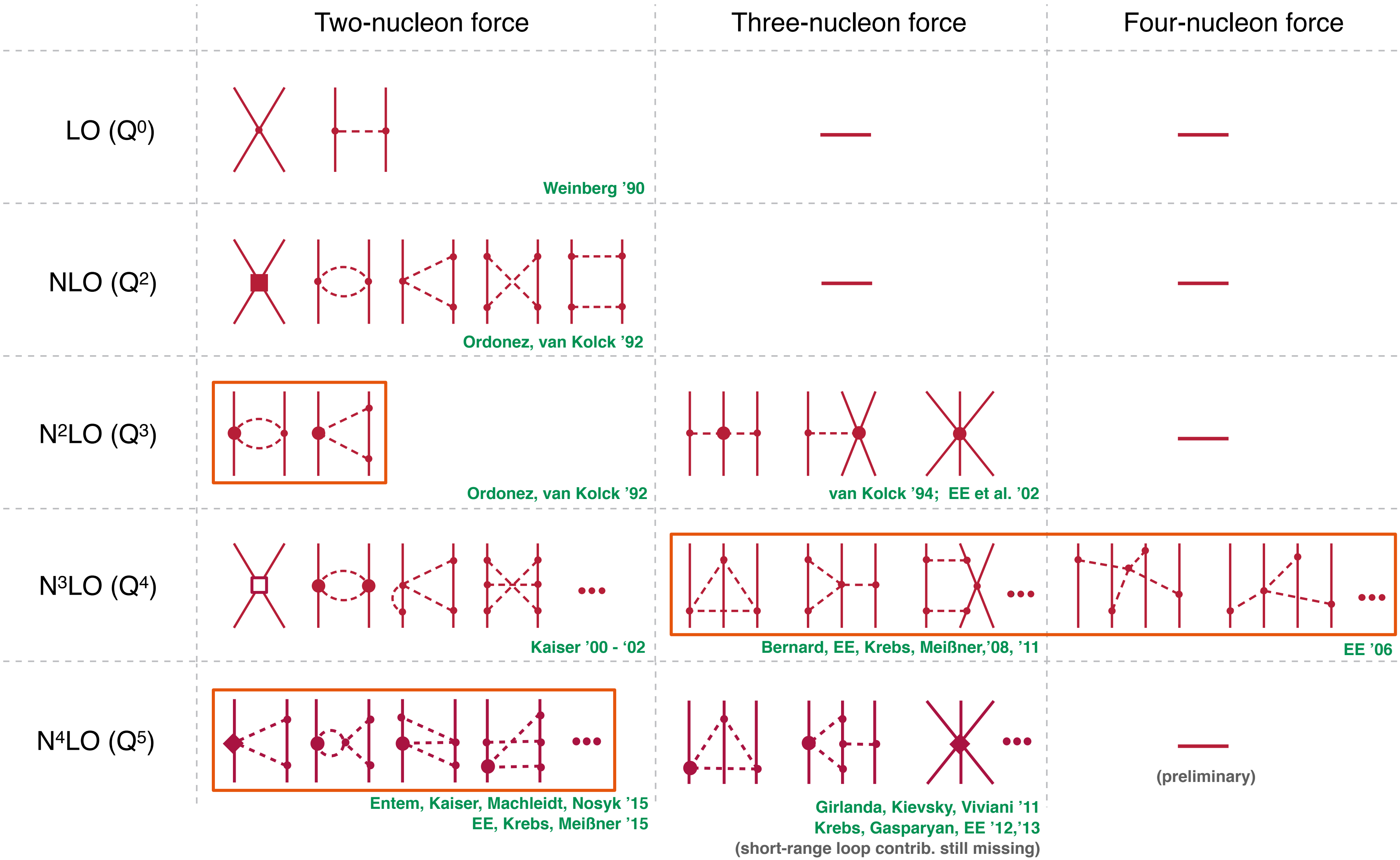

— long-range interactions are parameter-free predictions (all πN LECs known)

— all expressions are derived using dimensional regularization of loop integrals

Regularization

One has to introduce a regulator with $\Lambda \sim \Lambda_b$. In practice, low values of Λ are preferable:

— many-body methods require soft interactions,

— spurious deeply-bound states for $\Lambda > \Lambda^{crit}$ make calculations for $A > 3$ unfeasible…

⟶ it is crucial to employ a regulator that minimizes finite-Λ artifacts!

Regularization

One has to introduce a regulator with $\Lambda \sim \Lambda_b$. In practice, low values of Λ are preferable:

- many-body methods require soft interactions,
- spurious deeply-bound states for $\Lambda > \Lambda^{\rm crit}$ make calculations for $A > 3$ unfeasible…

$\longrightarrow$ it is crucial to employ a regulator that minimizes finite-Λ artifacts!

Nonlocal: $V_{1\pi}^{\rm reg} \propto \dfrac{e^{-\frac{p'^4+p^4}{\Lambda^4}}}{\vec q^{\,2}+M_\pi^2} \longrightarrow \dfrac{1}{\vec q^{\,2}+M_\pi^2} \underbrace{\left(1-\dfrac{p'^4+p^4}{\Lambda^4}+\mathcal{O}(\Lambda^{-8})\right)}_{\text{affect long-range interactions...}}$

EE, Glöckle, Meißner '04;
Entem, Machleidt '03;
Entem, Machleidt, Nosyk '17; …

Regularization

One has to introduce a regulator with $\Lambda \sim \Lambda_b$. In practice, low values of Λ are preferable:

— many-body methods require soft interactions,
— spurious deeply-bound states for $\Lambda > \Lambda^{crit}$ make calculations for $A > 3$ unfeasible…

$\longrightarrow$ it is crucial to employ a regulator that minimizes finite-Λ artifacts!

Nonlocal: $$V_{1\pi}^{\rm reg} \propto \frac{e^{-\frac{p'^4+p^4}{\Lambda^4}}}{\vec q^{\,2}+M_\pi^2} \longrightarrow \frac{1}{\vec q^{\,2}+M_\pi^2}\underbrace{\left(1-\frac{p'^4+p^4}{\Lambda^4}+\mathcal{O}(\Lambda^{-8})\right)}_{\text{affect long-range interactions…}}$$

EE, Glöckle, Meißner ’04;
Entem, Machleidt ’03;
Entem, Machleidt, Nosyk ’17; …

Local: [inspired by Thomas Rijken] $$V_{1\pi}^{\rm reg} \propto \frac{e^{-\frac{\vec q^{\,2}+M_\pi^2}{\Lambda^2}}}{\vec q^{\,2}+M_\pi^2} \longrightarrow \frac{1}{\vec q^{\,2}+M_\pi^2}\left(1+\text{short-range terms}\right)$$

Reinert, Krebs, EE ’18;

$\longrightarrow$ does not affect long-range physics **at any order** in $1/\Lambda^2$-expansion

— Application to 2π exchange does not require re-calculating the corresponding diagrams:

$$V(q)=\frac{2}{\pi}\int_{2M_\pi}^\infty \mu\, d\mu \frac{\rho(\mu)}{q^2+\mu^2}+\ldots \xrightarrow{\text{reg.}} V_\Lambda(q)=e^{-\frac{q^2}{2\Lambda^2}}\frac{2}{\pi}\int_{2M_\pi}^\infty \mu\, d\mu \frac{\rho(\mu)}{q^2+\mu^2}e^{-\frac{\mu^2}{2\Lambda^2}}+\underbrace{\ldots}_{\text{polynomial in } q^2,\, M_\pi}$$

— Convention: choose polynomial terms such that $\Delta^n V_{\Lambda,\,\rm long}(\vec r)\big|_{r=0}=0$

Regularization

Regularized 2π-exchange potential (central isospin-dependent part of 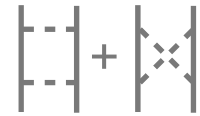):

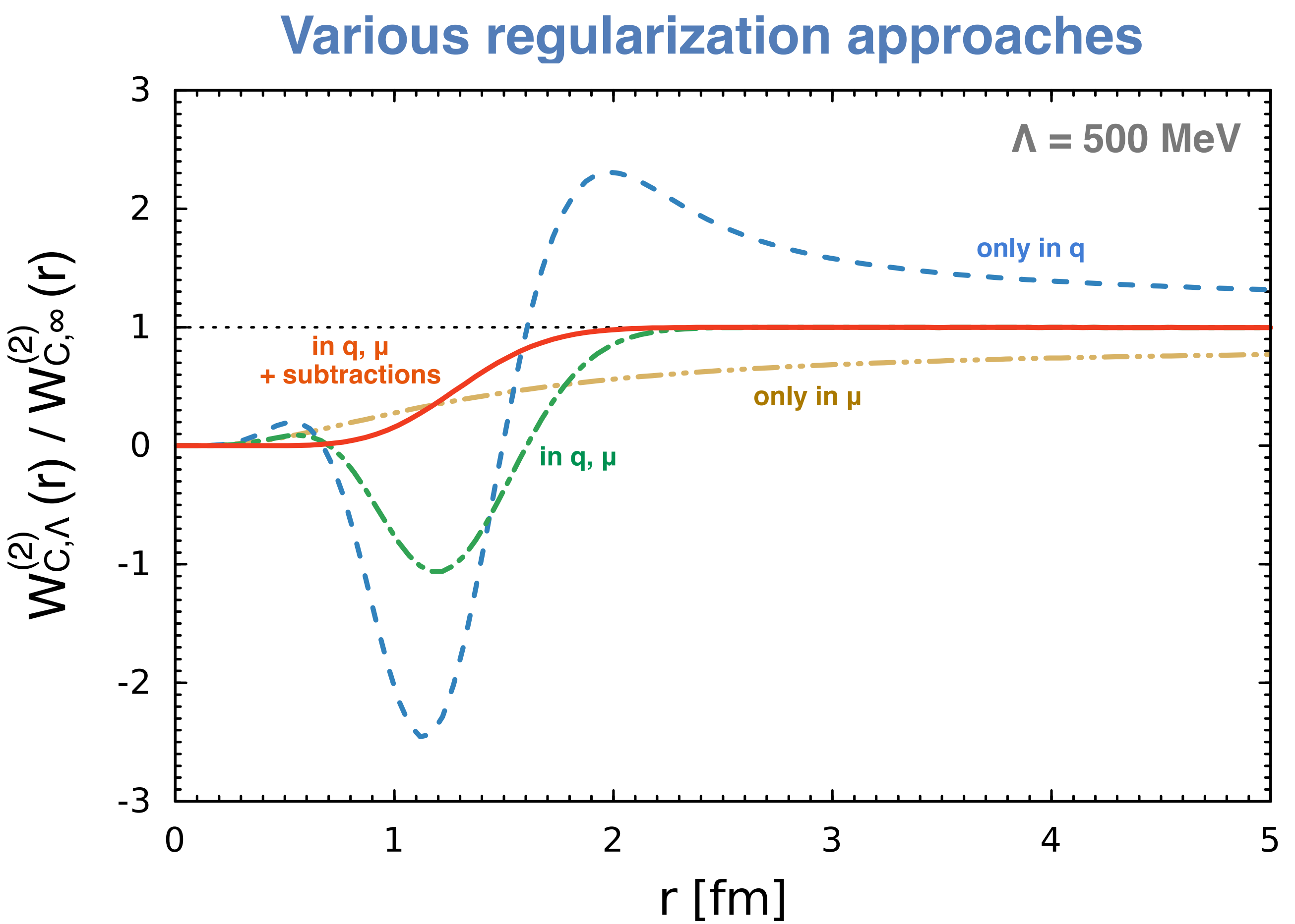

$$V(q) = \frac{2}{\pi}\int_{2M_\pi}^{\infty} \mu\, d\mu \frac{\rho(\mu)}{q^2+\mu^2} + \ldots \quad \xrightarrow{\text{reg.}} \quad V_\Lambda(q) = e^{-\frac{q^2}{2\Lambda^2}}\, \frac{2}{\pi}\int_{2M_\pi}^{\infty} \mu\, d\mu \frac{\rho(\mu)}{q^2+\mu^2}\, e^{-\frac{\mu^2}{2\Lambda^2}} + \ldots$$

Description of NN data

- The newest Bochum NN potentials up to N^{4}LO$^+$ provide a perfect description of mutually consistent NN data up to the pion production threshold Reinert, Krebs, EE, EPJA (18); PRL 126 (21) 092501

high-precision „realistic“ potentials				*Idaho χEFT*		*Bochum SMS χEFT ('21)*	
Nijm I	Nijm II	Reid93	CD Bonn	$\mathrm{N^4LO^+_{450}}$	$\mathrm{N^4LO^+_{500}}$	$\mathbf{N^4LO^+_{450}}$	$\mathbf{N^4LO^+_{500}}$
1.061	1.070	1.078	1.042	2.019	1.203	**1.013**	**1.015**

Description of NN data

- The newest Bochum NN potentials up to N⁴LO⁺ provide a perfect description of mutually consistent NN data up to the pion production threshold Reinert, Krebs, EE, EPJA (18); PRL 126 (21) 092501

high-precision „realistic" potentials				*Idaho χEFT*		*Bochum SMS χEFT ('21)*	
Nijm I	Nijm II	Reid93	CD Bonn	$N^4LO^+_{450}$	$N^4LO^+_{500}$	$\mathbf{N^4LO^+_{450}}$	$\mathbf{N^4LO^+_{500}}$
1.061	1.070	1.078	1.042	2.019	1.203	**1.013**	**1.015**

- A representative example: pp scattering observables at E_{lab} = 143 MeV

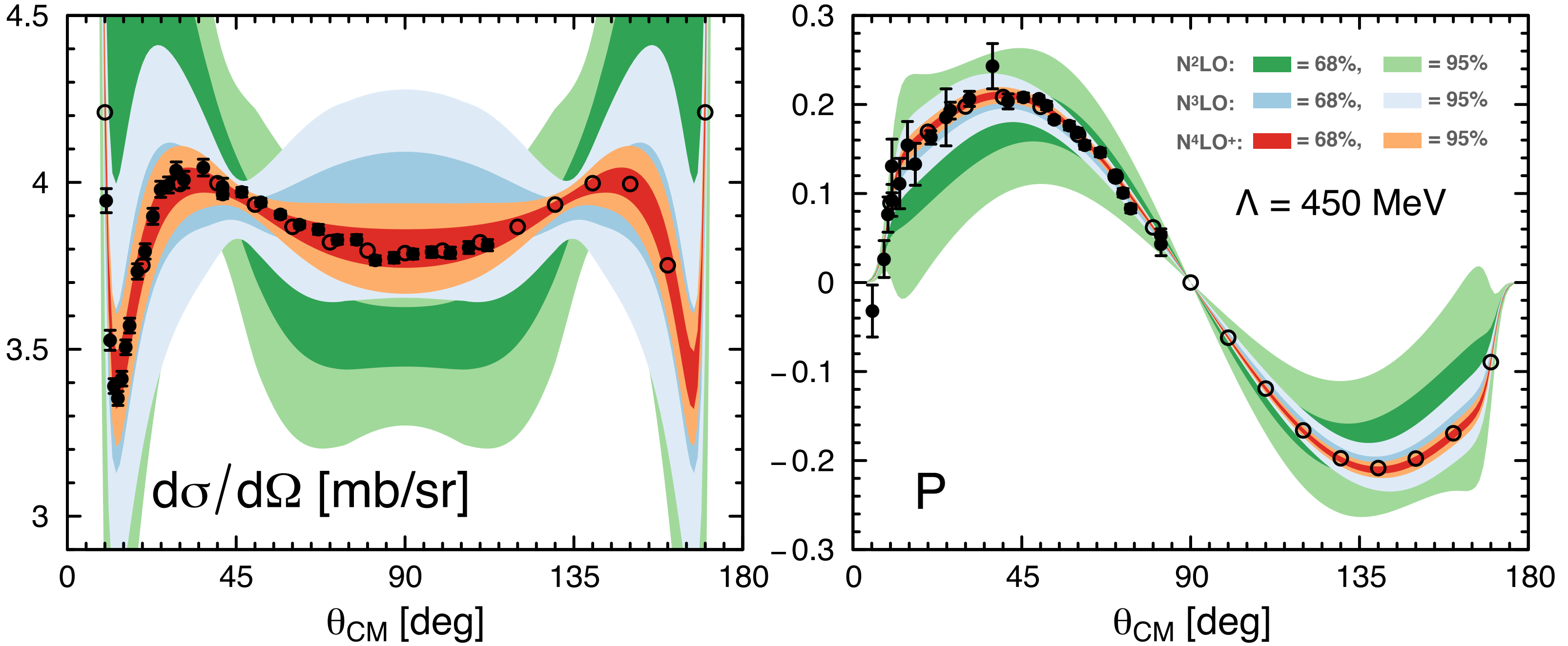

Residual regulator dependence

χ^2/datum for the description of the NN data in the range of 0 – 200 MeV at N^{4}LO$^+$

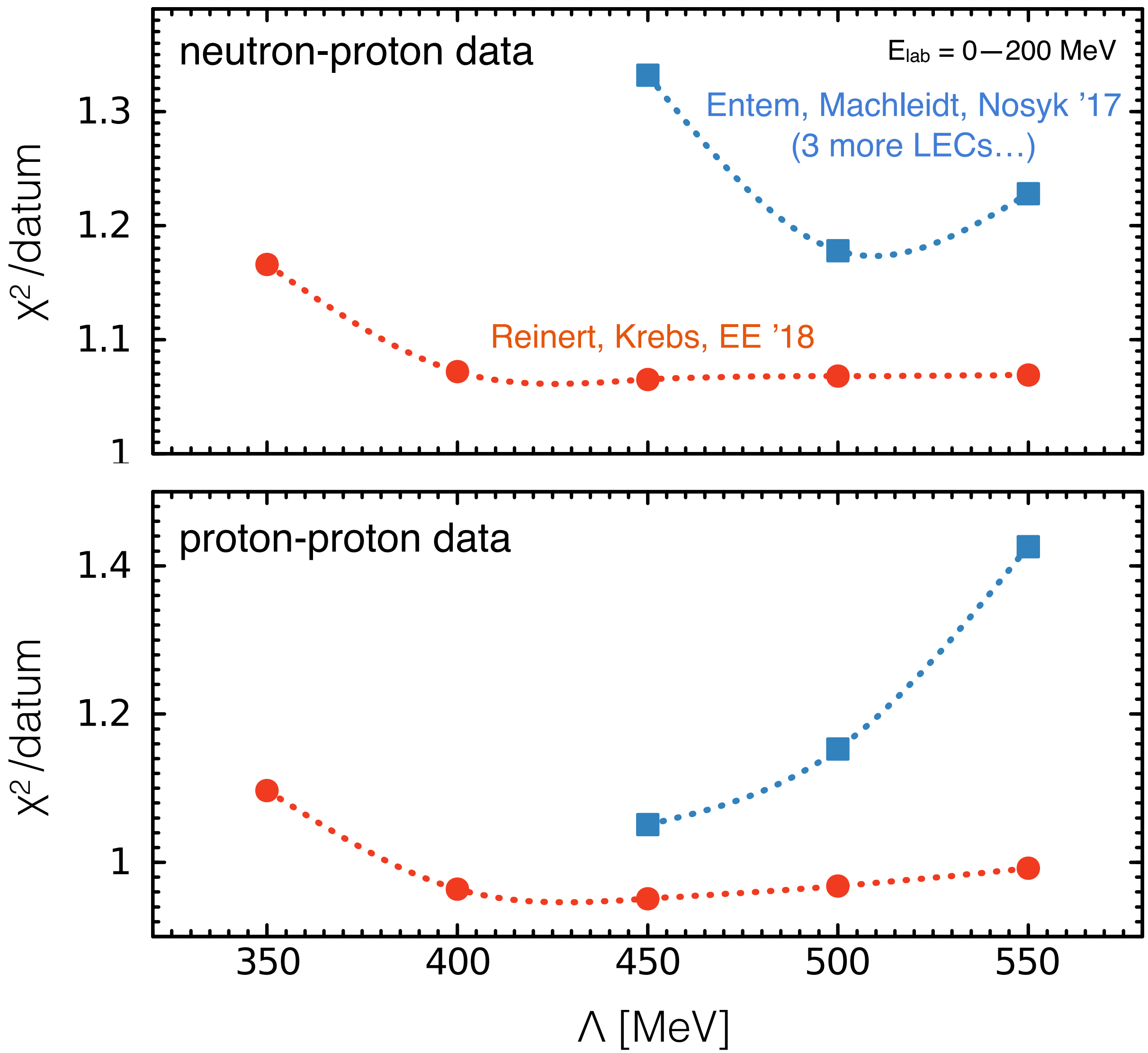

Few-nucleon systems at N^{2}LO

The leading contribution to the 3NF (Q^3, N^{2}LO):

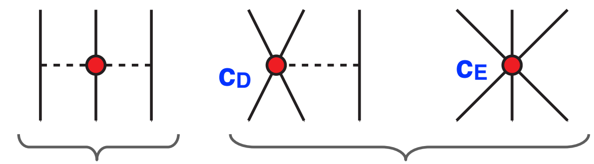

parameter-free

fixed from 3N data:

— ^{3}H binding energy

— Nd cross section minimum at 70 MeV [K. Sekiguchi et al.'02]

$\Rightarrow$ test the χEFT Hamiltonian, fixed in $A \leq 3$ systems, in heavier nuclei

LENPIC: Low **E**nergy **N**uclear **P**hysics **I**nternational **C**ollaboration

Predictions for Nd total cross section

Maris et al. [LENPIC], e-Print: 2206.13303; to appear in PRC

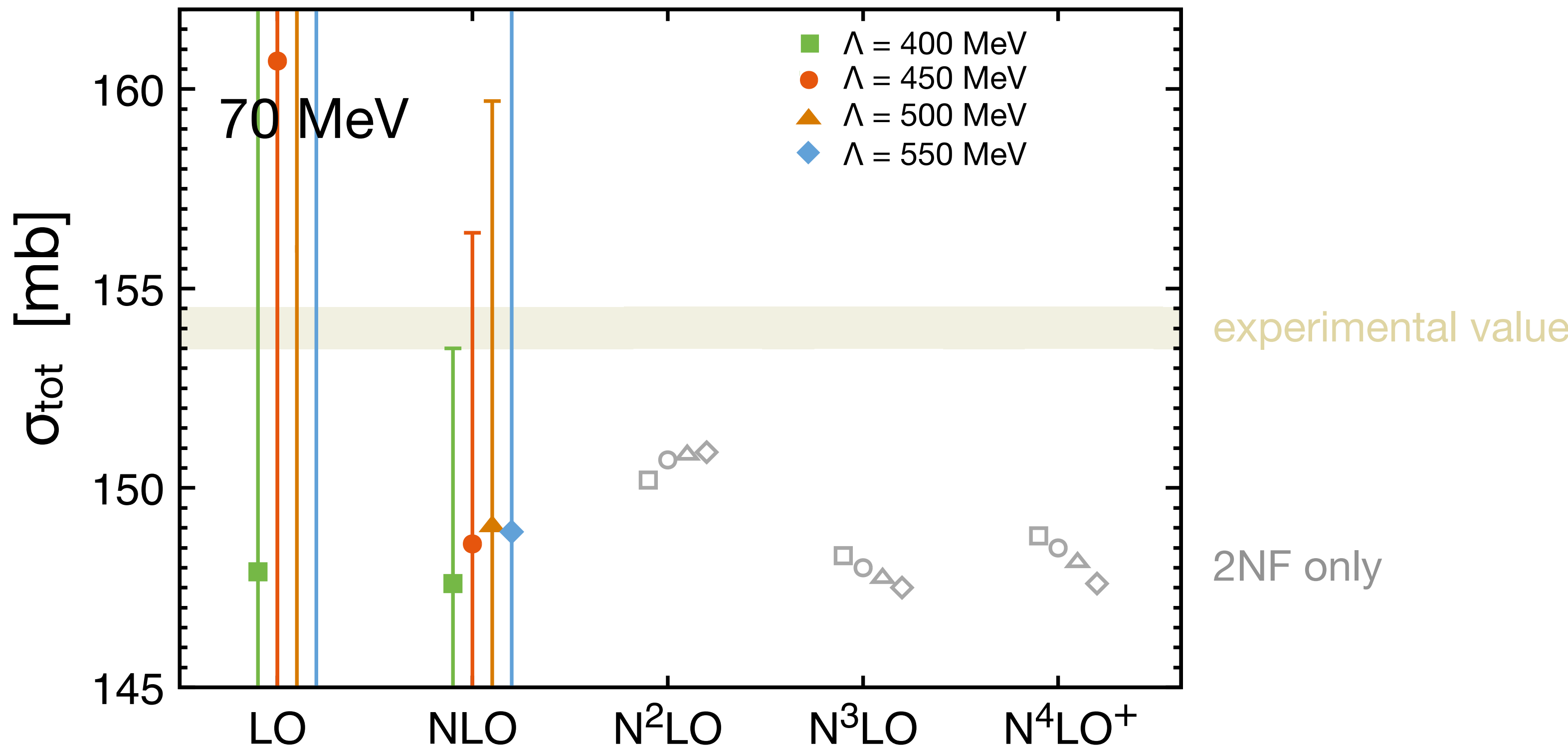

— 2NF only underestimates the data; adding the 3NF improves the agreement with exp.

— 3NF contributions of natural size (W. counting)

— small residual cutoff dependence

Predictions for Nd total cross section

Maris et al. [LENPIC], e-Print: 2206.13303; to appear in PRC

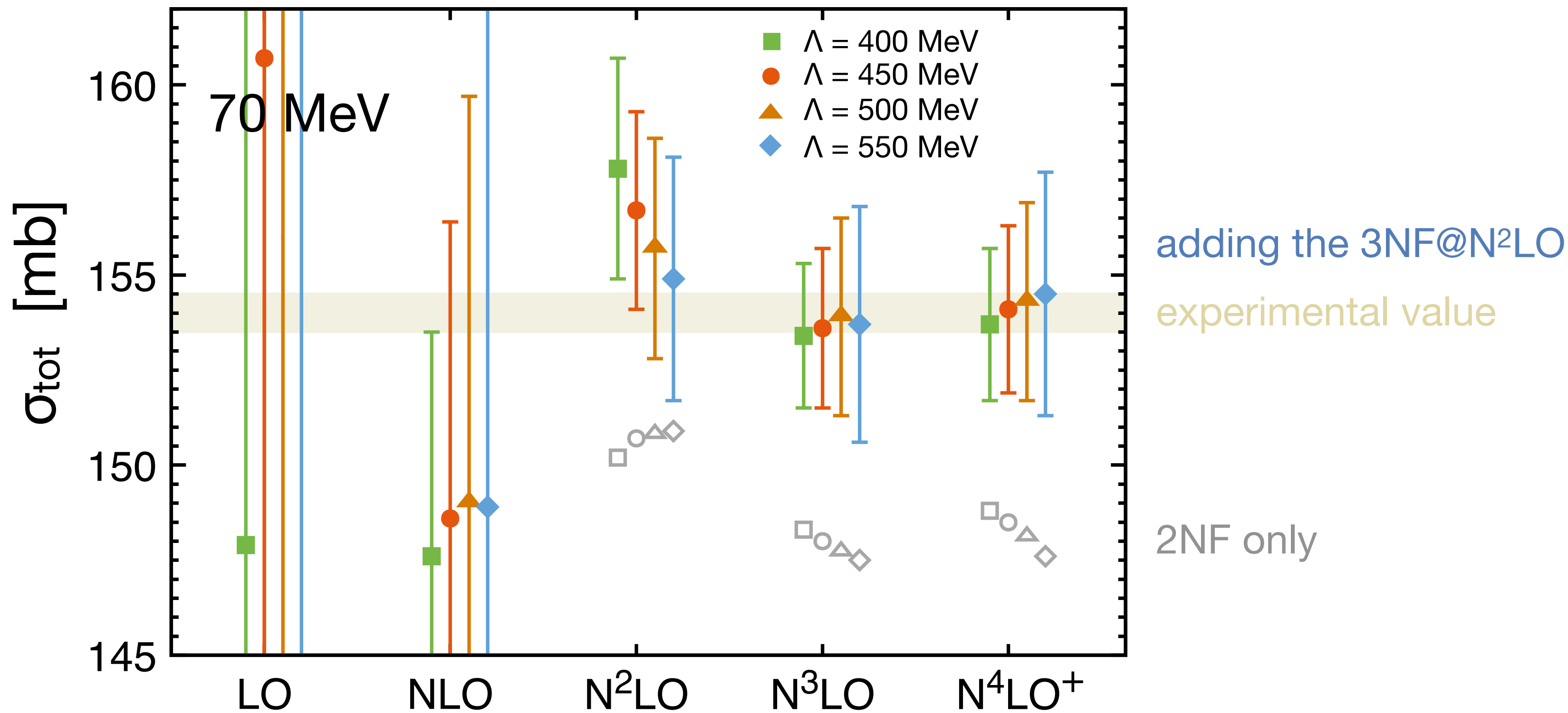

— 2NF only underestimates the data; adding the 3NF improves the agreement with exp.

— 3NF contributions of natural size (W. counting)

— small residual cutoff dependence

LENPIC: Low Energy Nuclear Physics International Collaboration

Few-N systems and light nuclei to N^{2}LO

P. Maris et al. (LENPIC), Phys. Rev. C 103 (2021) 5, 054001

Tensor analyzing powers in Nd elastic scattering at 70 MeV

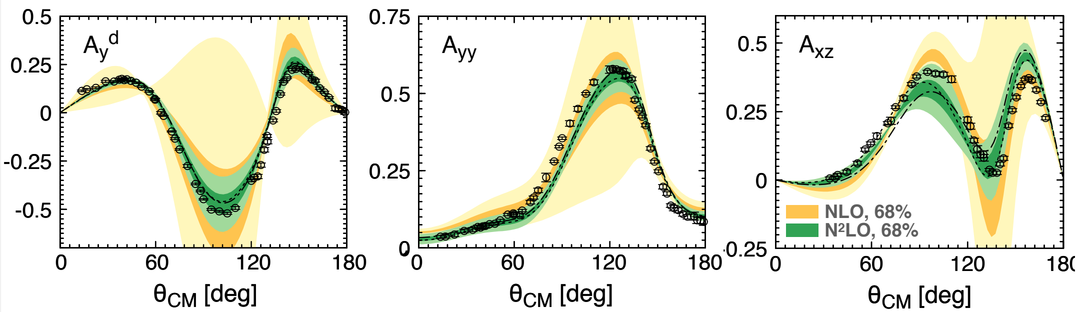

Predictions for ground-state energies of light nuclei

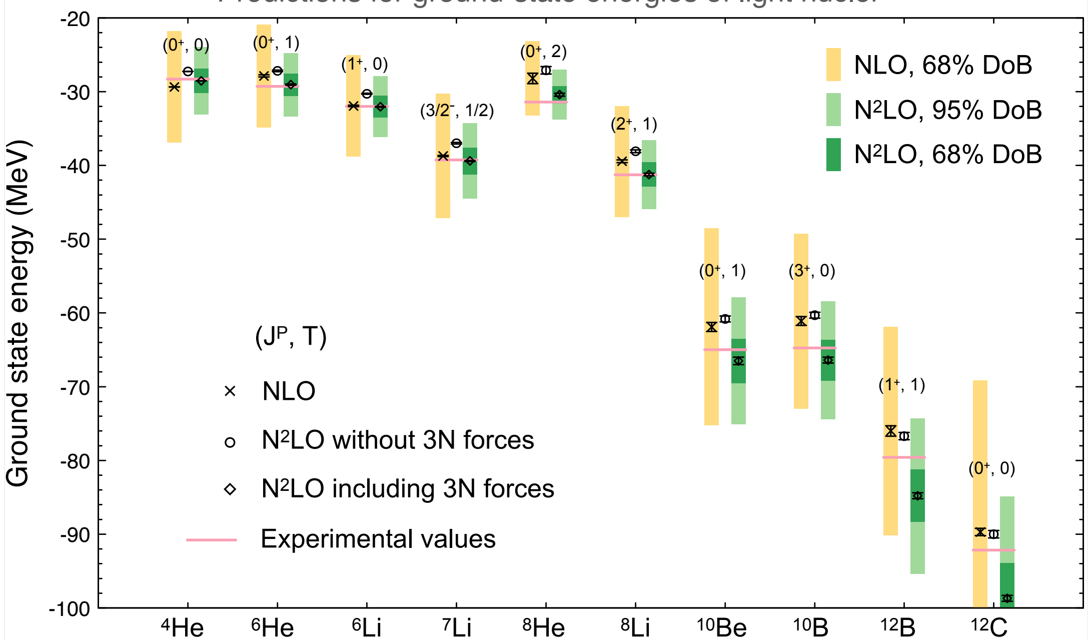

Excitation energies

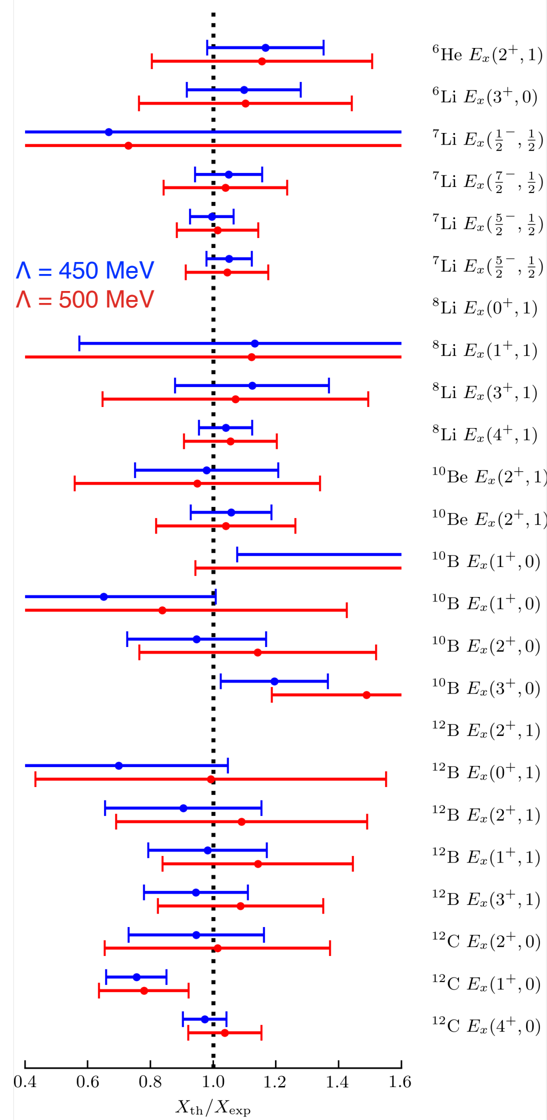

Few-N systems and light nuclei to N²LO

P. Maris et al. (LENPIC), Phys. Rev. C 103 (2021) 5, 054001

Tensor analyzing powers in Nd elastic scattering at 70 MeV

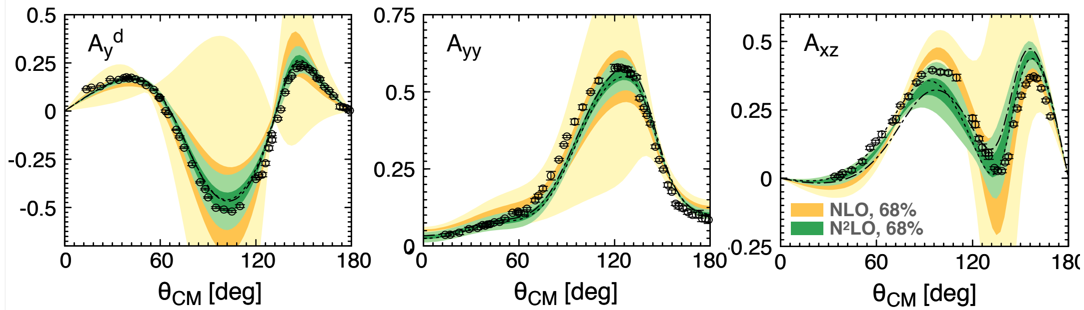

Predictions for ground-state energies of light nuclei

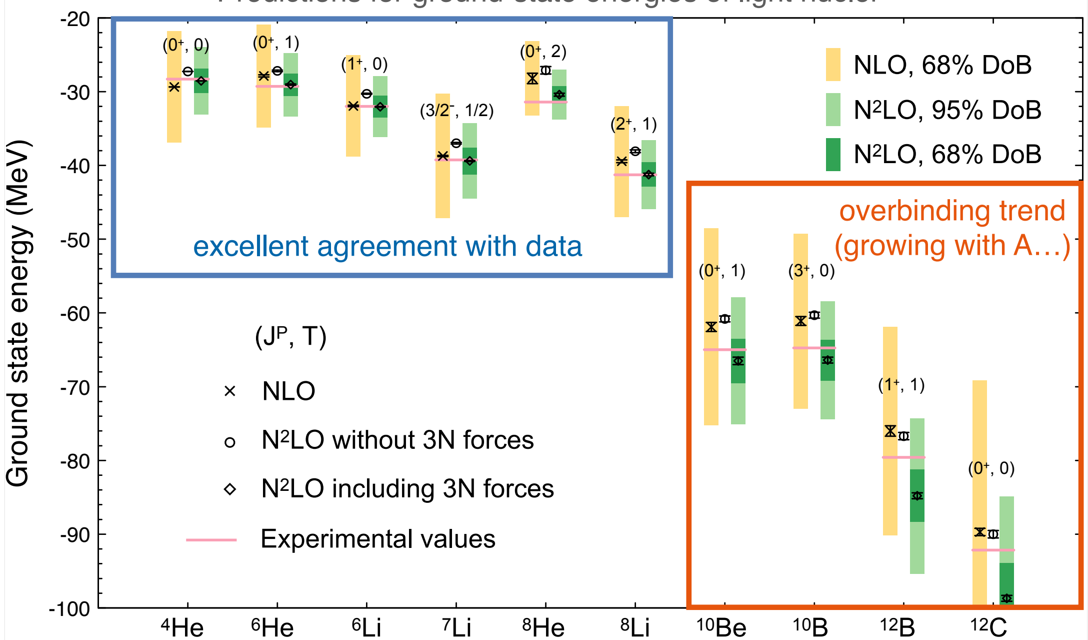

Excitation energies

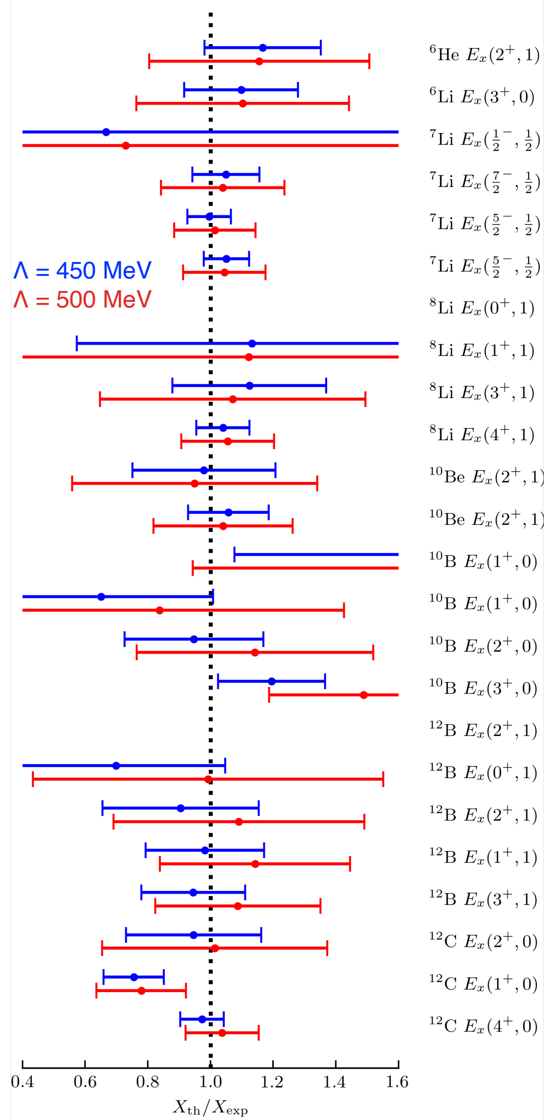

Few-N systems and light nuclei to N²LO

P. Maris et al. (LENPIC), e-Print: 2206.13303 [nucl-th], to appear in PRC

LENPIC

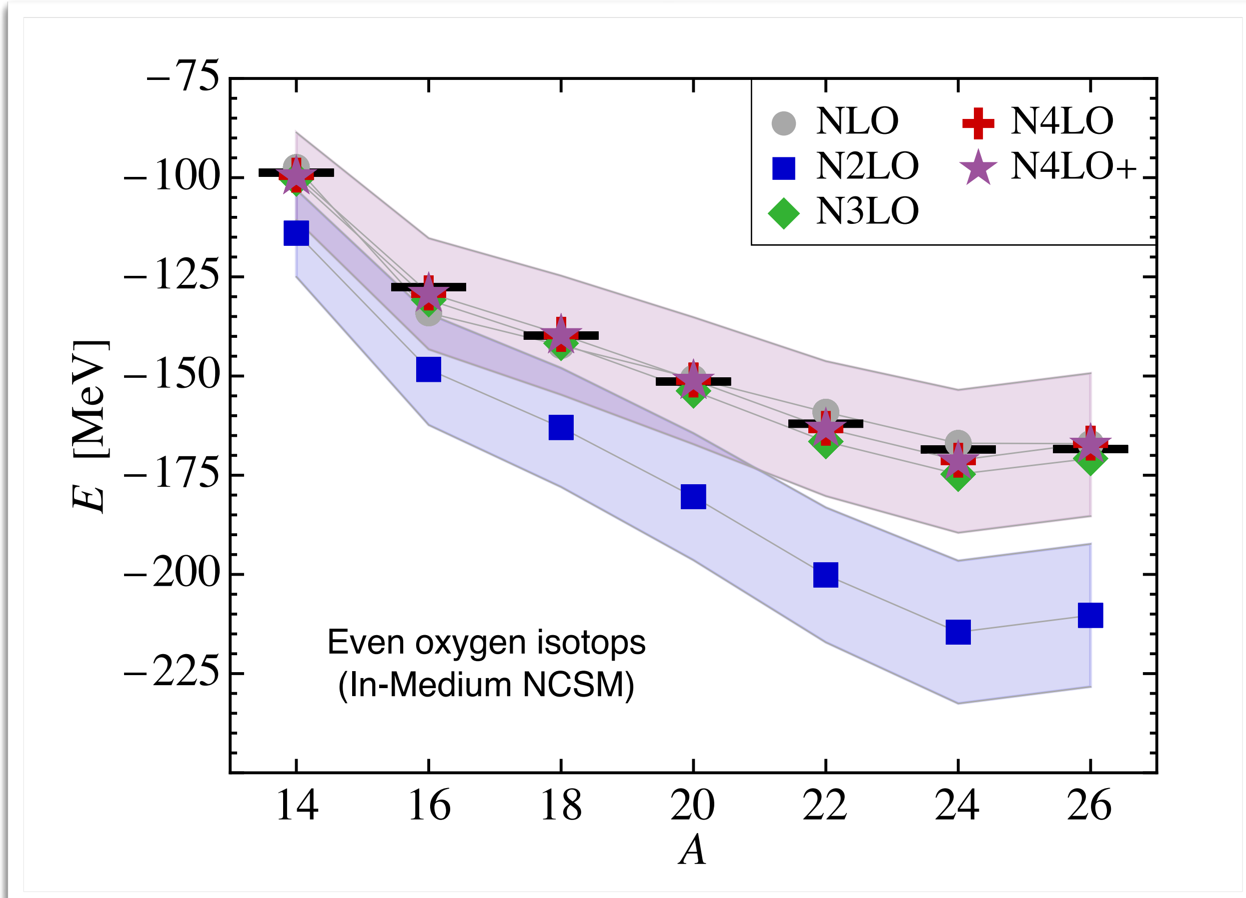

A remarkable predictive power!

Few-N systems and light nuclei to N²LO

P. Maris et al. (LENPIC), e-Print: 2206.13303 [nucl-th], to appear in PRC

LENPIC

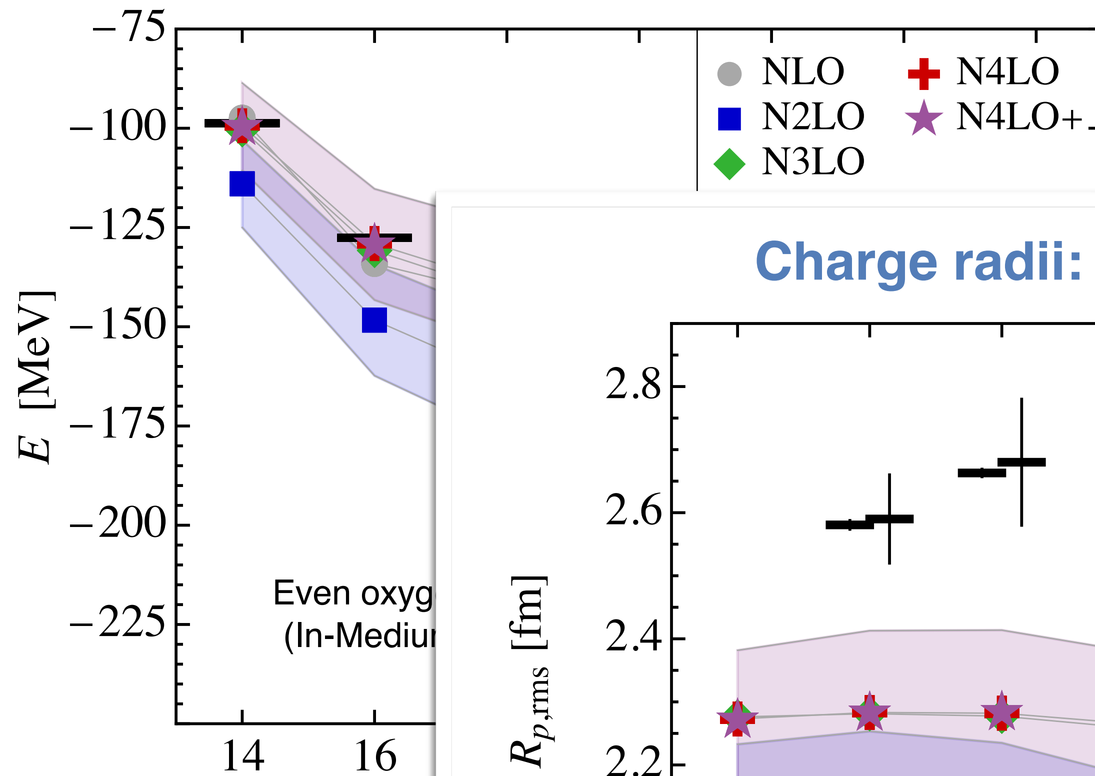

A remarkable predictive power!

Charge radii: A smoking gun?

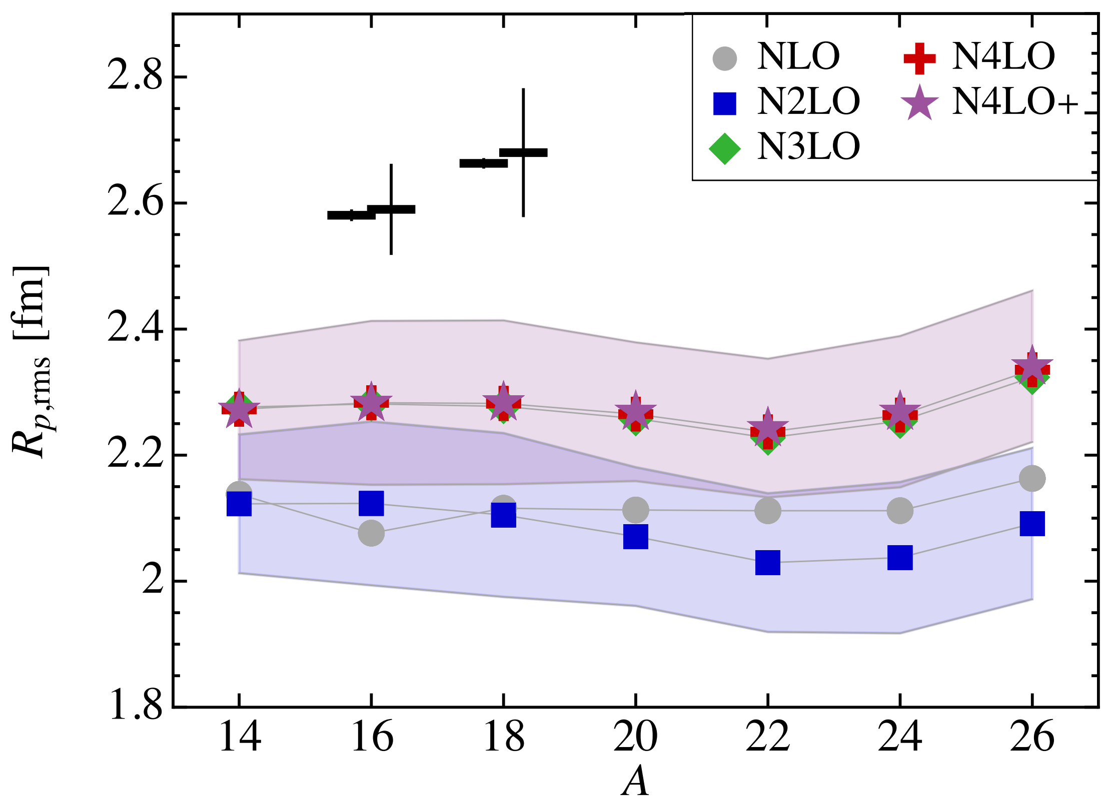

Precision determination of charge radii of light nuclei

Filin, Baru, EE, Krebs, Möller, Reinert, PRL 124 (2020) 082501;
Filin, Möller, Baru, EE, Krebs, Reinert, PRC 103 (2021) 024313;
Filin, Baru, EE, Körber, Krebs, Möller, Reinert, in preparation

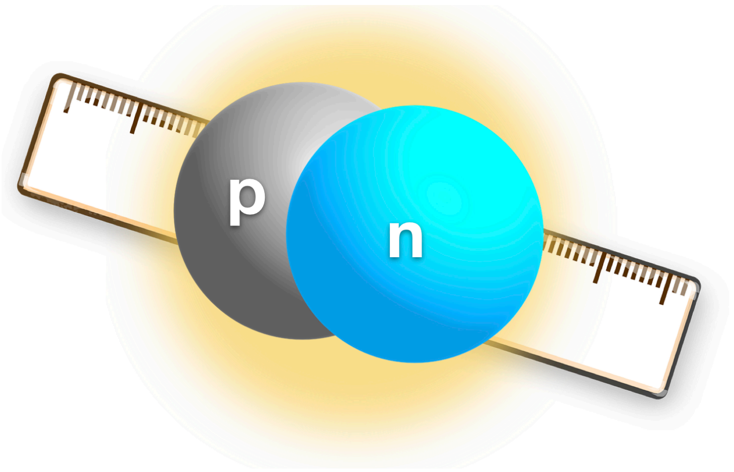

Precision determinations of charge radii of light nuclei

The charge radii are defined as a slope of the charge form factor G_C:

$$r_C^2 = (-6)\frac{\partial G_C(Q^2)}{\partial Q^2}\bigg|_{Q^2=0}$$

What we calculate in the structure radius, which incorporates all nuclear effects:

$$r_C^2 = r_{str}^2 + \left(r_p^2 + \frac{3}{4m_p^2}\right) + \frac{A-Z}{Z} r_n^2$$

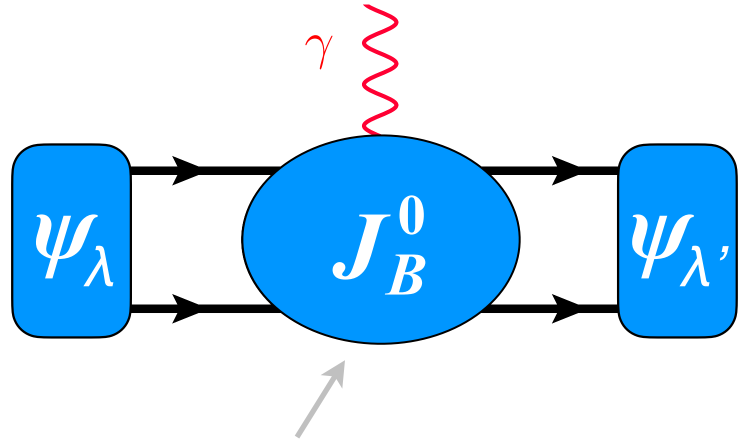

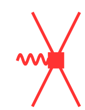

isoscalar charge density available to N⁴LO (3 LECs)

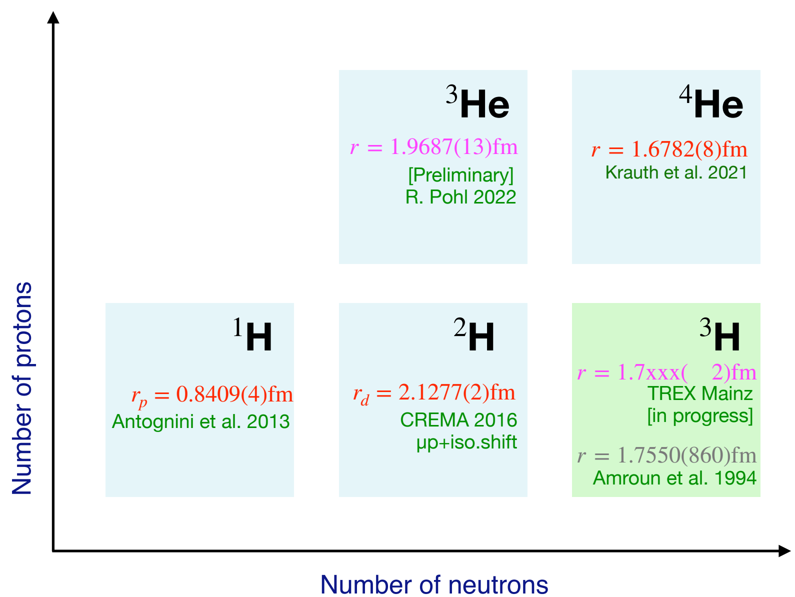

Motivation:

- underpredicted radii for medium-mass nuclei found by LENPIC
- new source of information on r_p, r_n (provided nuclear effects under control)
- precision tests of chiral EFT

Deuteron charge and quadrupole FFs

Filin, Möller, Baru, EE, Krebs, Reinert, PRL 124 (2020) 082501; PRC 103 (2021) 024313

The charge and quadrupole form factors of the deuteron at N⁴LO

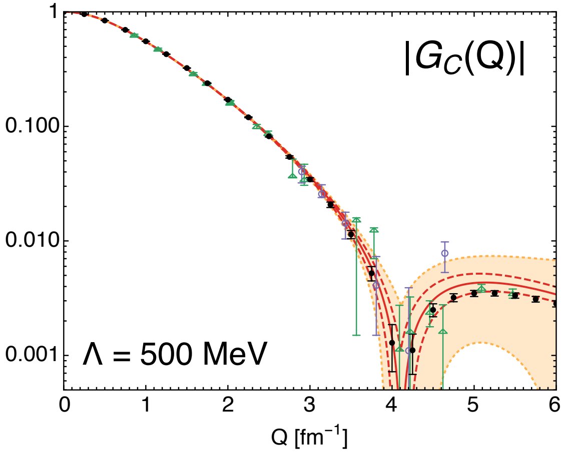

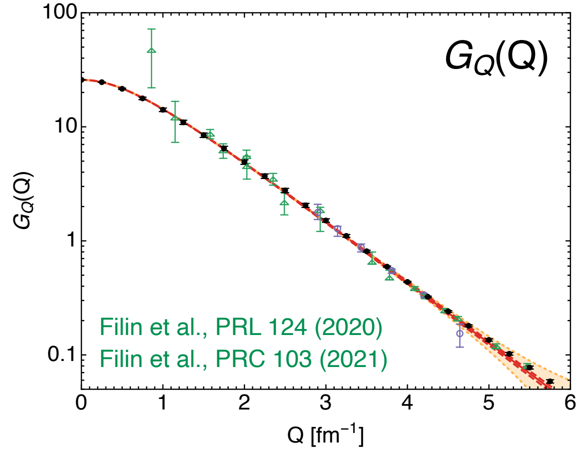

The extracted structure radius and quadrupole moment:

$$r_{\rm str} = 1.9729^{+0.0015}_{-0.0012}\ \text{fm}$$

$$Q_{\rm d} = 0.2854^{+0.0038}_{-0.0017}\ \text{fm}^2$$

statistical and systematic errors due to the EFT truncation, choice of fitting range and πN LECs

The value of $Q_{\rm d}$ is to be compared with $Q_{\rm d}^{\rm exp} = 0.285\,699(15)(18)$ fm^2 Puchalski et al., PRL 125 (2020)

Deuteron charge and quadrupole FFs

Filin, Möller, Baru, EE, Krebs, Reinert, PRL 124 (2020) 082501; PRC 103 (2021) 024313

The charge and quadrupole form factors of the deuteron at N⁴LO

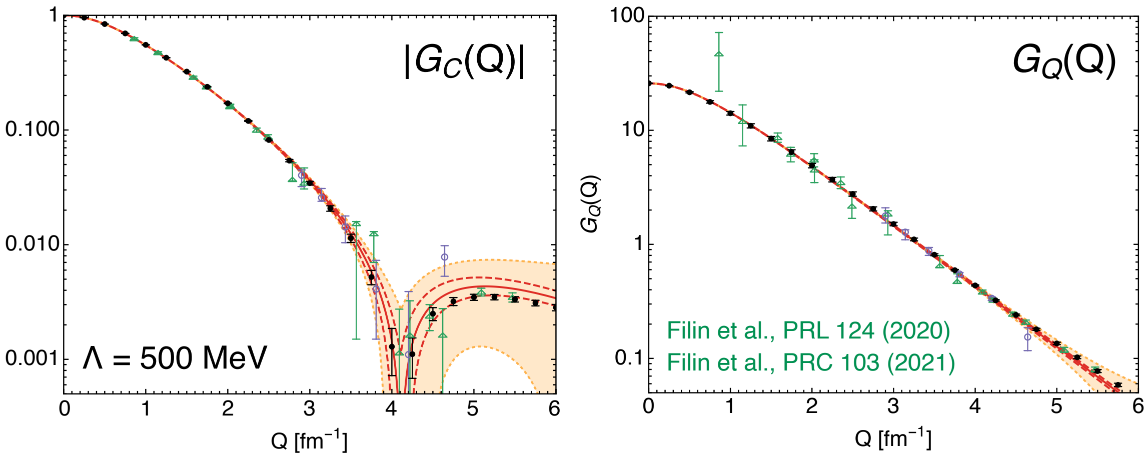

The extracted structure radius and quadrupole moment:

$$r_{\rm str} = 1.9729^{+0.0015}_{-0.0012}\ \text{fm}$$

$$Q_{\rm d} = 0.2854^{+0.0038}_{-0.0017}\ \text{fm}^2$$

statistical and systematic errors due to the EFT truncation, choice of fitting range and πN LECs

The value of $Q_{\rm d}$ is to be compared with $Q_{\rm d}^{\rm exp} = 0.285\,699(15)(18)$ fm^2 Puchalski et al., PRL 125 (2020)

Combining our result for $r_{\rm str}^2 = r_d^2 - r_p^2 - r_n^2 - \dfrac{3}{4m_p^2}$ with the

¹H-²H isotope shift datum $r_d^2 - r_p^2 = 3.82070(31)$ fm^2 leads

to the prediction for the neutron radius:

$$\boxed{r_n^2 = -\,0.105^{+0.005}_{-0.006}\ \text{fm}^2}$$

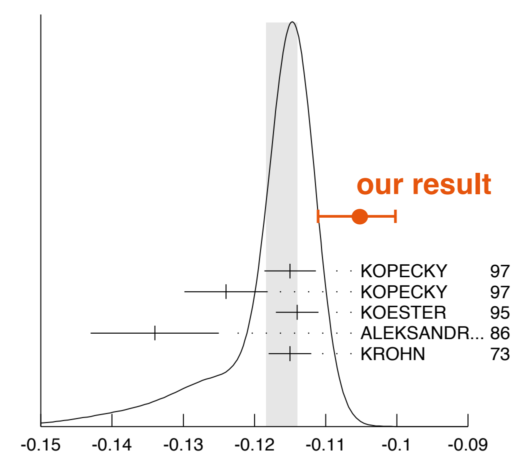

Deuteron charge and quadrupole FFs

Filin, Möller, Baru, EE, Krebs, Reinert, PRL 124 (2020) 082501; PRC 103 (2021) 024313

The charge and quadrupole form factors of the deuteron at N⁴LO

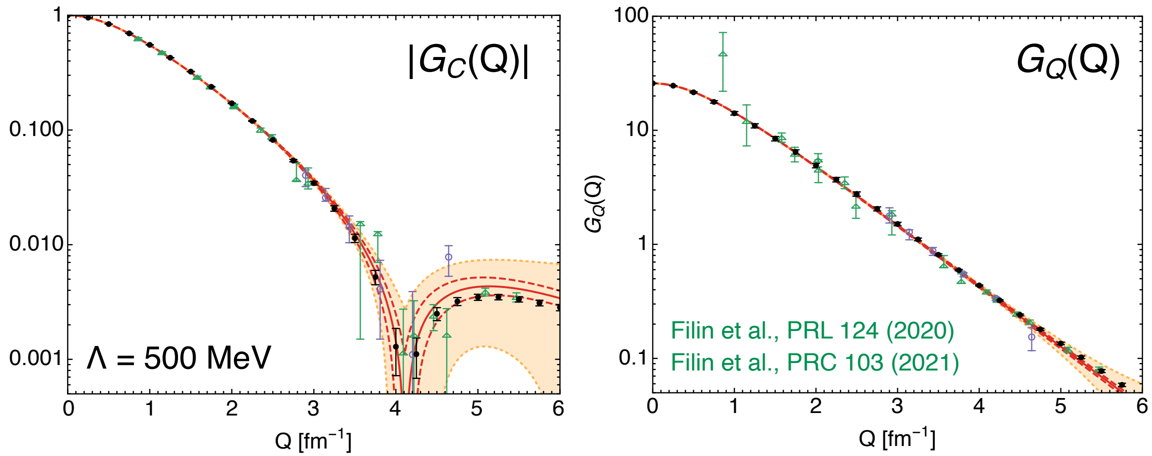

The extracted structure radius and quadrupole moment:

$$r_{\rm str} = 1.9729^{+0.0015}_{-0.0012}\ \text{fm}$$

$$Q_{\rm d} = 0.2854^{+0.0038}_{-0.0017}\ \text{fm}^2$$

statistical and systematic errors due to the EFT truncation, choice of fitting range and πN LECs

The value of $Q_{\rm d}$ is to be compared with $Q_{\rm d}^{\rm exp} = 0.285\,699(15)(18)\ \text{fm}^2$ Puchalski et al., PRL 125 (2020)

Combining our result for $r_{\rm str}^2 = r_d^2 - r_p^2 - r_n^2 - \dfrac{3}{4m_p^2}$ with the ¹H-²H isotope shift datum $r_d^2 - r_p^2 = 3.82070(31)\ \text{fm}^2$ leads to the prediction for the neutron radius:

$$\boxed{r_n^2 = -\,0.105^{+0.005}_{-0.006}\ \text{fm}^2}$$

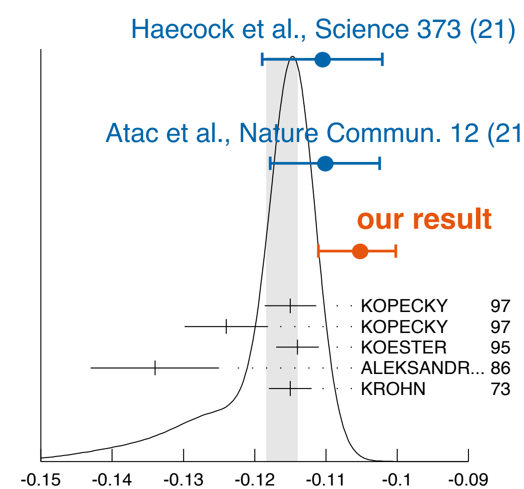

A = 3,4 nuclei (preliminary)

Charge radius of ^{4}He

2 out of 3 LECs in the short-range 2N charge density already fixed from the ^{2}H FFs; the remaining one is determined from the ^{4}He FF

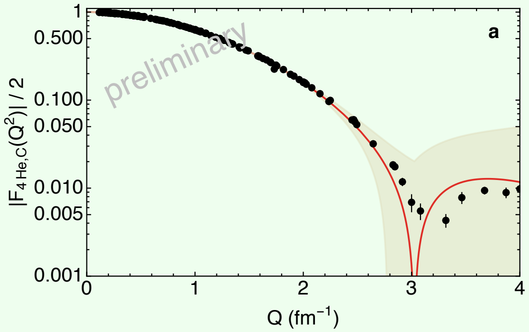

$\Rightarrow$ $\boxed{r_C(^4\mathrm{He}) = 1.6798 \pm 0.0035\, fm}$

using CODATA r_p and own determination of r_n

Experimental value (μ^{4}He): $r_C^{\mathrm{exp}}(^4\mathrm{He}) = (1.67824 \pm 0.00083)$ fm

A = 3,4 nuclei (preliminary)

Charge radius of ^{4}He

2 out of 3 LECs in the short-range 2N charge density already fixed from the ^{2}H FFs; the remaining one is determined from the ^{4}He FF

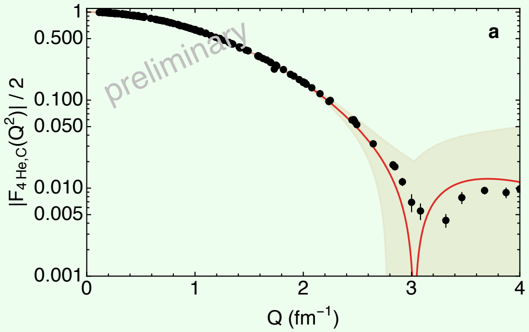

$$\Rightarrow \quad \boxed{r_C(^4\text{He}) = 1.6798 \pm 0.0035 \, fm}$$

using CODATA r_p and own determination of r_n

Experimental value (μ^{4}He): $r_C^{\text{exp}}(^4\text{He}) = (1.67824 \pm 0.00083)$ fm Krauth et al., Nature 589 (2021) 7843, 527-531

A = 3,4 nuclei (preliminary)

Charge radius of ^{4}He

2 out of 3 LECs in the short-range 2N charge density already fixed from the ^{2}H FFs; the remaining one is determined from the ^{4}He FF

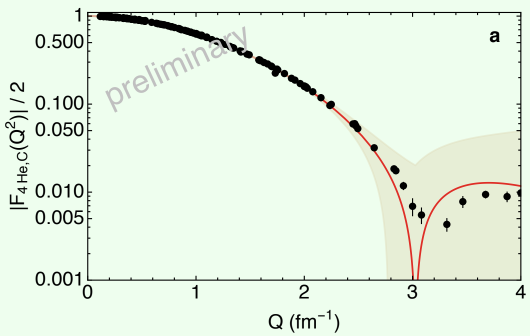

$$\Rightarrow \boxed{r_C(^4\mathrm{He}) = 1.6798 \pm 0.0035\; fm}$$

using CODATA r_p and own determination of r_n

Experimental value (μ^{4}He): $r_C^{\mathrm{exp}}(^4\mathrm{He}) = (1.67824 \pm 0.00083)$ fm Krauth et al., Nature 589 (2021) 7843, 527-531

Parameter-free prediction of the iso-scalar 3N charge radius

$$\boxed{r_C(3N_{\mathrm{isoscalar}}) \;\equiv\; \sqrt{1/3\, r_C^2(^3\mathrm{H}) \;+\; 2/3\, \mathrm{r}_C^2(^3\mathrm{He})} \;=\; (1.9058 \pm 0.0026)\; fm}$$

preliminary, using CODATA-2018 r_p and own determination of r_n

Experimental value: $r_C^{\mathrm{exp}}(3N_{\mathrm{isoscalar}}) = (1.903 \pm 0.029)\; fm$ (limited by the ^{3}H value)

Amroun et al. ’94 (world average e$^-$ on ^{3}H); Pohl ’22 (μ^{3}He)

A = 3,4 nuclei (preliminary)

Charge radius of ⁴He

2 out of 3 LECs in the short-range 2N charge density already fixed from the ^{2}H FFs; the remaining one is determined from the ^{4}He FF

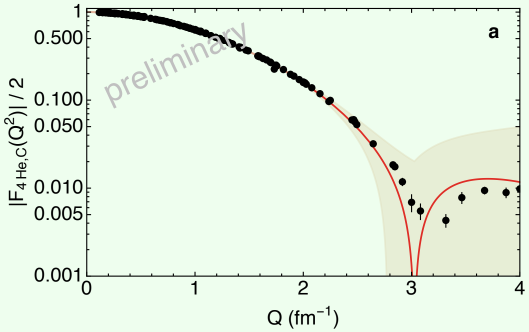

$$\Rightarrow \quad \boxed{r_C(^4\text{He}) = 1.6798 \pm 0.0035\, fm}$$

using CODATA r_p and own determination of r_n

Experimental value (μ⁴He): $r_C^{\exp}(^4\text{He}) = (1.67824 \pm 0.00083)$ fm Krauth et al., Nature 589 (2021) 7843, 527-531

Parameter-free prediction of the iso-scalar 3N charge radius

$$\boxed{r_C(3N_{\text{isoscalar}}) \equiv \sqrt{1/3\, r_C^2(^3\text{H}) + 2/3\, \text{r}_C^2(^3\text{He})} = (1.9058 \pm 0.0026)\, fm}$$

preliminary, using CODATA-2018 r_p and own determination of r_n

Experimental value: $r_C^{\exp}(3N_{\text{isoscalar}}) = (1.903 \pm 0.029)\, fm$ (limited by the ^{3}H value)

Amroun et al. ’94 (world average e⁻ on ^{3}H); Pohl ’22 (μ³He)

MEC contribution increases from ~0.3% for ^{2}H to ~3% for ^{4}He! Heavier nuclei in progress…

Towards solution of the 3NF challenge

- High-precision NN potentials V_{2N} describe NN data with $\chi^2/\text{datum} \sim 1$

- No Hamiltonian $H = H_{\text{kin}} + V_{2N} + V_{3N}$ exists that can describe Nd data, e.g.:

Energy	potential	A_y	iT_{11}	T_{20}	T_{21}	T_{22}
10 MeV	AV18	288	29	10	6.2	24
	AV18+UR	224	23	13	6.1	7.6

$\longleftarrow$ $\chi^2/\text{datum} \sim 1$

Alejandro Kievsky, in Tews et al., FBS 63 (22) 4, 67

3N scattering in chiral EFT

2N scattering

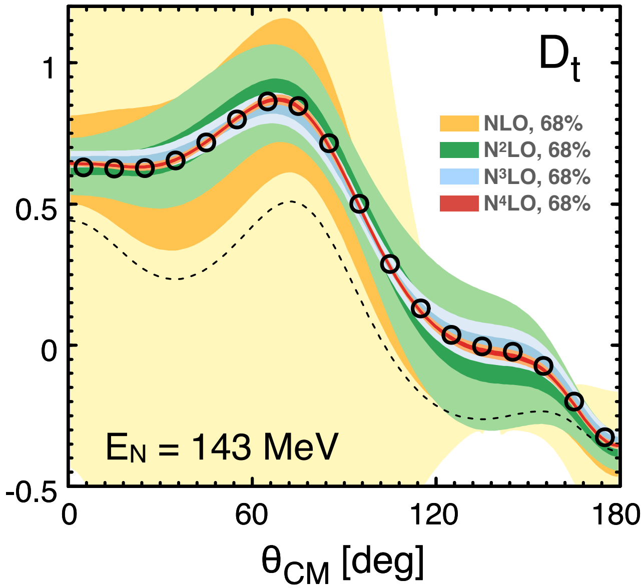

3N scattering

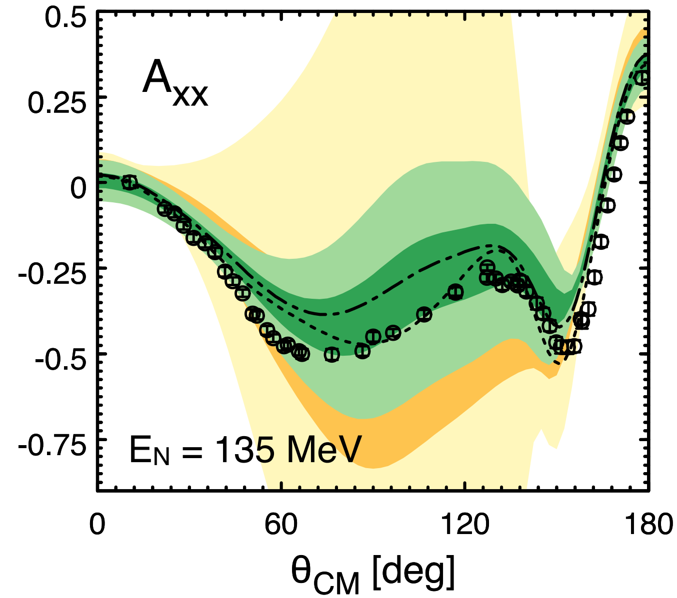

$\Rightarrow$ precise description of 3N data will likely require pushing chiral EFT for the 3NF to N^4LO

Challenges to be addressed:

— Conceptual: Consistent regularization of the 3NF beyond N^2LO

— Computational: Determination of $\gtrsim 15$ LECs in the 3NF at N^4LO

$$[\text{CPU time}]_{\text{3N amplitude}} \sim 10^7 \cdot [\text{CPU time}]_{\text{2N amplitude}}$$

3NF: the need for consistent regularization

Using DimReg to calculate loop diagrams in the 3NF + cutoff regularization in the dynamical equation violates the chiral symmetry

3NF: the need for consistent regularization

Using DimReg to calculate loop diagrams in the 3NF + cutoff regularization in the dynamical equation violates the chiral symmetry

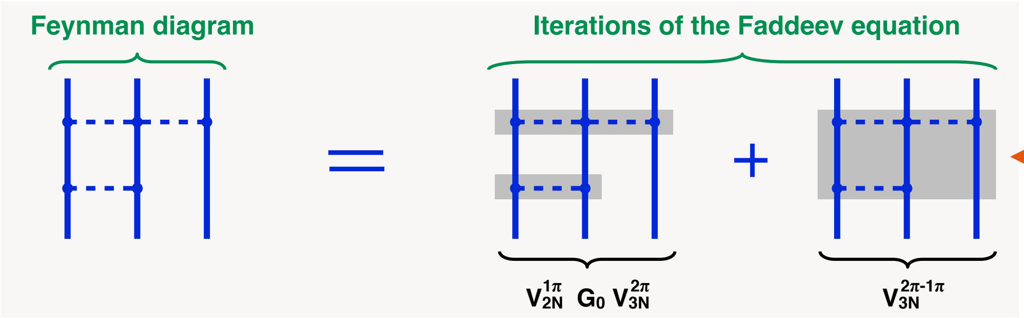

3NF calculated using DimReg
Betrard, EE, Krebs, Meißner '08

- Using DimReg everywhere: l.h.s. = r.h.s. $\Rightarrow$ consistent

3NF: the need for consistent regularization

Using DimReg to calculate loop diagrams in the 3NF + cutoff regularization in the dynamical equation violates the chiral symmetry

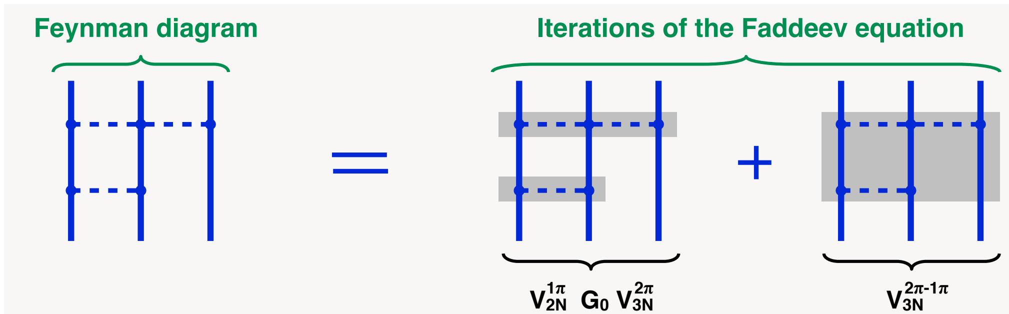

3NF calculated using DimReg
Betrard, EE, Krebs, Meißner '08

- Using DimReg everywhere: l.h.s. = r.h.s. $\Rightarrow$ consistent
- Calculate the iterative diagram on the r.h.s. using cutoff regularization:

$$V_{2N,\,\Lambda}^{1\pi}\, G_0\, V_{3N,\,\Lambda}^{2\pi} = -\,\Lambda \frac{g_A^4}{96\sqrt{2\pi^3}F_\pi^6}\left[\underbrace{\tau_1\cdot\tau_3\,(\vec{q}_3\cdot\vec{\sigma}_1)}_{\text{absorbable into } c_D} - \underbrace{\frac{4}{3}(\tau_2\cdot\tau_3-\tau_1\cdot\tau_3)(\vec{q}_2\cdot\vec{\sigma}_3)}_{\text{violates chiral symmetry...}}\right]\frac{\vec{q}_3\cdot\vec{\sigma}_3}{q_3^3+M_\pi^2} + \ldots$$

absorbable into c_D: 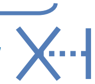

violates chiral symmetry...

3NF: the need for consistent regularization

Using DimReg to calculate loop diagrams in the 3NF + cutoff regularization in the dynamical equation violates the chiral symmetry

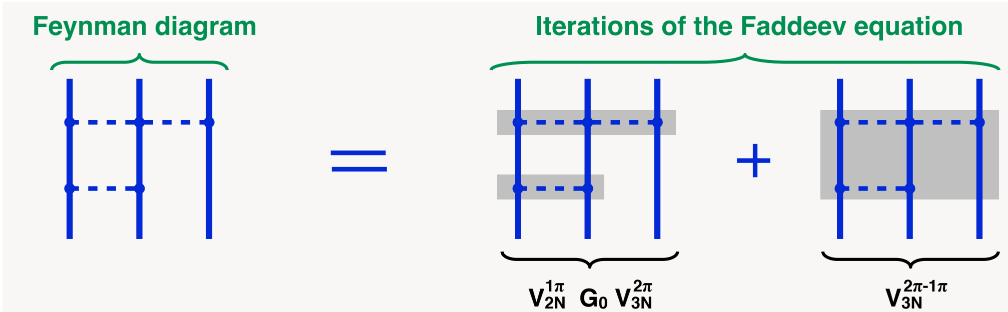

- Using DimReg everywhere: l.h.s. = r.h.s. $\Rightarrow$ consistent
- Calculate the iterative diagram on the r.h.s. using cutoff regularization:

$$V_{2N,\,\Lambda}^{1\pi}\, G_0\, V_{3N,\,\Lambda}^{2\pi} = -\Lambda \frac{g_A^4}{96\sqrt{2\pi^3}F_\pi^6}\Big[\underbrace{\tau_1\cdot\tau_3\,(\vec{q}_3\cdot\vec{\sigma}_1)}_{\text{absorbable into } c_D} - \underbrace{\frac{4}{3}(\tau_2\cdot\tau_3-\tau_1\cdot\tau_3)(\vec{q}_2\cdot\vec{\sigma}_3)}_{\text{violates chiral symmetry...}}\Big]\frac{\vec{q}_3\cdot\vec{\sigma}_3}{q_3^3+M_\pi^2} + \ldots$$

- The problematic divergence cancels if $V_{3N}^{2\pi-1\pi}$ is calculated using cutoff regularization.

3NF: the need for consistent regularization

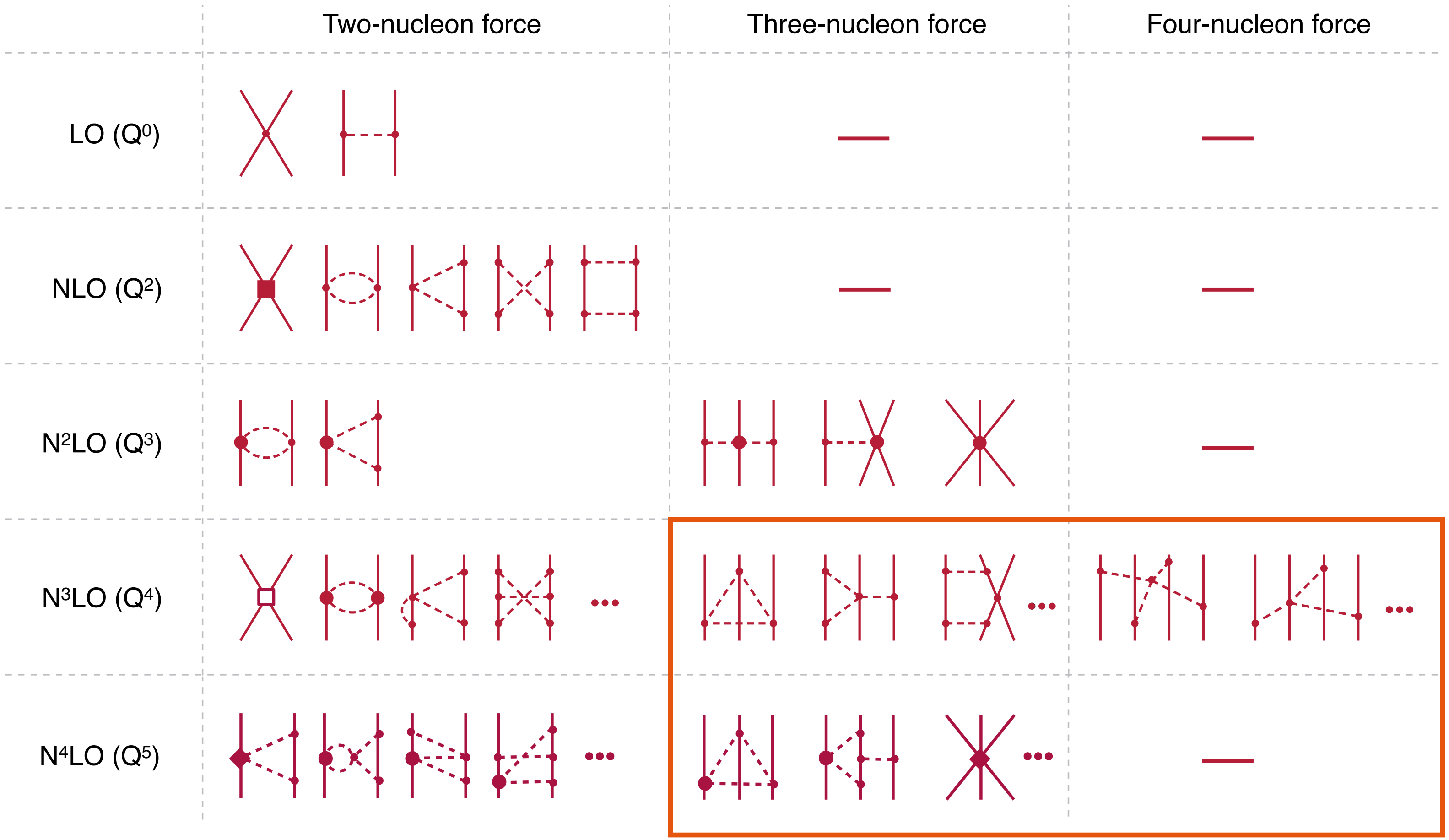

⇒ 3NF and currents beyond N^{2}LO must be re-derived using symmetry-preserving regulator

— e.g., the higher-derivative [Slavnov ’71] or gradient flow regularization [Lüscher ’10]

— a new path-integral approach to derive nuclear forces and currents [Krebs, EE, in preparation]

Example: gradient flow reg. of the 4NF

Consider e.g. the contribution to the 4NF at N³LO involving a 4π-vertex:

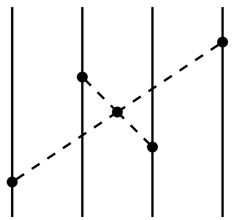

Unregularized expression:

EE, PLB 639 (2006) 456; EPJA 34 (2007) 197

$$V_{4\mathrm{N}} = \frac{g_A^4}{2(2F_\pi)^6} \frac{\vec{\sigma}_1 \cdot \vec{q}_1 \; \vec{\sigma}_2 \cdot \vec{q}_2 \; \vec{\sigma}_3 \cdot \vec{q}_3 \; \vec{\sigma}_4 \cdot \vec{q}_4}{(\vec{q}_1^{\,2} + M_\pi^2)\,(\vec{q}_2^{\,2} + M_\pi^2)\,(\vec{q}_3^{\,2} + M_\pi^2)\,(\vec{q}_4^{\,2} + M_\pi^2)} \Big[\big(\vec{q}_1 + \vec{q}_2\big)^2 + M_\pi^2 \Big]$$

$$+ \text{ 3-pole terms} + \text{all permutations}$$

Example: gradient flow reg. of the 4NF

Consider e.g. the contribution to the 4NF at N³LO involving a 4π-vertex:

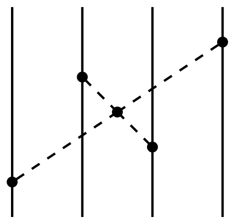

Unregularized expression:

EE, PLB 639 (2006) 456; EPJA 34 (2007) 197

$$V_{4\mathrm{N}} = \frac{g_A^4}{2(2F_\pi)^6} \frac{\vec{\sigma}_1 \cdot \vec{q}_1 \; \vec{\sigma}_2 \cdot \vec{q}_2 \; \vec{\sigma}_3 \cdot \vec{q}_3 \; \vec{\sigma}_4 \cdot \vec{q}_4}{(\vec{q}_1^{\,2} + M_\pi^2)\,(\vec{q}_2^{\,2} + M_\pi^2)\,(\vec{q}_3^{\,2} + M_\pi^2)\,(\vec{q}_4^{\,2} + M_\pi^2)} \Big[(\vec{q}_1 + \vec{q}_2)^2 + M_\pi^2 \Big]$$

$$+ \text{ 3-pole terms } + \text{ all permutations}$$

Applying the gradient flow regularization method consistent with the 2NF yields:

Hermann Krebs, EE, preliminary

$$V_{4\mathrm{N}} = \frac{g_A^4}{2(2F_\pi)^6} \frac{\vec{\sigma}_1 \cdot \vec{q}_1 \; \vec{\sigma}_2 \cdot \vec{q}_2 \; \vec{\sigma}_3 \cdot \vec{q}_3 \; \vec{\sigma}_4 \cdot \vec{q}_4}{(\vec{q}_1^{\,2} + M_\pi^2)\,(\vec{q}_2^{\,2} + M_\pi^2)\,(\vec{q}_3^{\,2} + M_\pi^2)\,(\vec{q}_4^{\,2} + M_\pi^2)} \Big[(\vec{q}_1 + \vec{q}_2)^2 + M_\pi^2 \Big]$$

$$\times \left(4\, e^{-\frac{\vec{q}_2^{\,2} + M_\pi^2}{\Lambda^2}}\, e^{-\frac{\vec{q}_3^{\,2} + M_\pi^2}{\Lambda^2}}\, e^{-\frac{\vec{q}_4^{\,2} + M_\pi^2}{\Lambda^2}} \; - \; 3\, e^{-\frac{\vec{q}_1^{\,2} + M_\pi^2}{2\Lambda^2}}\, e^{-\frac{\vec{q}_2^{\,2} + M_\pi^2}{2\Lambda^2}}\, e^{-\frac{\vec{q}_3^{\,2} + M_\pi^2}{2\Lambda^2}}\, e^{-\frac{\vec{q}_4^{\,2} + M_\pi^2}{2\Lambda^2}} \right)$$

$$+ \text{ 3-pole terms } + \text{ all permutations}$$

Computational challenge: Eigenvector continuation

Consider a Hamiltonian $\hat{H}(\vec{C})$ that depends on continuously varying LECs $\vec{C} = (C_1, C_2, \ldots, C_N)$.

EC = variational method that allows to compute GS energy E and state $|\Psi_{\mathrm{gs}}\rangle$ of $\hat{H}(\vec{C})$ by projecting it onto the „training“ states $|\Psi_{\mathrm{gs}}^{(i)}\rangle,\ \hat{H}(\vec{C}_i)|\Psi_{\mathrm{gs}}^{(i)}\rangle = E_{\mathrm{gs}}^{(i)}|\Psi_{\mathrm{gs}}^{(i)}\rangle$ Lee, Frame, Ekström, König, …

$\Rightarrow$ generalized eigenvalue problem on a low-dim subspace $\{|\Psi_{\mathrm{gs}}^{(1)}\rangle, |\Psi_{\mathrm{gs}}^{(2)}\rangle, \ldots, |\Psi_{\mathrm{gs}}^{(d)}\rangle\}$

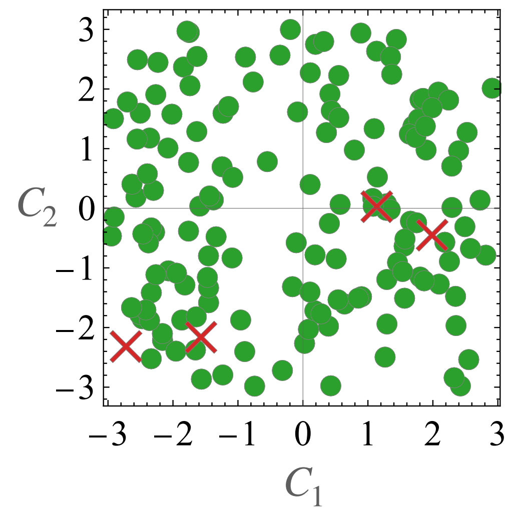

Has been successfully applied to medium-mass nuclei, 2-particle scattering [Furnstahl et al.’20] and even to 3-particle scattering [Zhang et al.’21].

Computational challenge: Eigenvector continuation

Consider a Hamiltonian $\hat{H}(\overrightarrow{C})$ that depends on continuously varying LECs $\overrightarrow{C} = (C_1, C_2, \ldots, C_N)$.

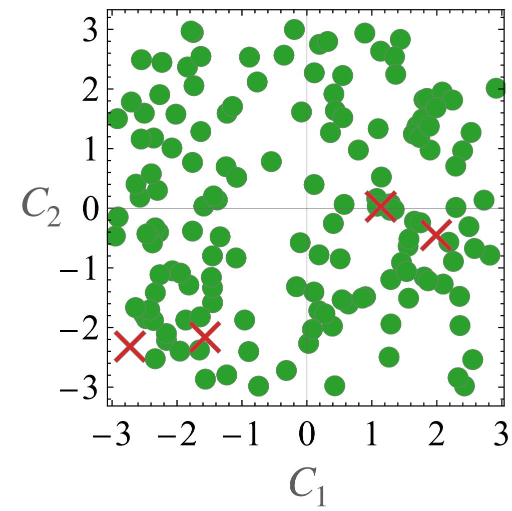

EC = variational method that allows to compute GS energy E and state $|\Psi_{\rm gs}\rangle$ of $\hat{H}(\overrightarrow{C})$ by projecting it onto the „training" states $|\Psi_{\rm gs}^{(i)}\rangle$, $\hat{H}(\overrightarrow{C}_i)|\Psi_{\rm gs}^{(i)}\rangle = E_{\rm gs}^{(i)}|\Psi_{\rm gs}^{(i)}\rangle$ Lee, Frame, Ekström, König, …

$\Rightarrow$ generalized eigenvalue problem on a low-dim subspace $\{|\Psi_{\rm gs}^{(1)}\rangle, |\Psi_{\rm gs}^{(2)}\rangle, \ldots, |\Psi_{\rm gs}^{(d)}\rangle\}$

Has been successfully applied to medium-mass nuclei, 2-particle scattering [Furnstahl et al.'20] and even to 3-particle scattering [Zhang et al.'21].

2-particle scattering as a test (fixed partial wave l and energy $E_{cms} = k^2/m$)

The task: compute $\delta(k)$ for $\hat{H}(\overrightarrow{C})$ without solving the LS equation for $\hat{H}(\overrightarrow{C})$ using some training scattering states or phase shifts $\delta^{(i)}(k)$ of $\hat{H}(\overrightarrow{C}_i)$ with $i = 1, \ldots, d$.

Can be achieved using the **Kohn variational principle** for scattering states [Furnstahl et al.,'20].

Eigenvector continuation

Adapting Furnstahl et al., PLB 809 (20) 135719 to momentum space leads to the following procedure (fixed k):

1) calculate d half-shell K-matrices $K_{pk}^{(i)}$ (conventions: $S = 1 - 2imkT_{kk},\ \ 1/K_{pk} = \mathrm{Re}(1/T_{pk})$)

2) calculate the $d \times d$ matrix $(\Delta U)_{ij}$:

$$(\Delta U)_{ij} = \underbrace{V_{kk}^{(ij)}}_{\hat{V}^{(ij)} \equiv 2\hat{V}(\vec{C}) - \hat{V}(\vec{C}_i) - \hat{V}(\vec{C}_j)} + \frac{2m}{\pi} \int p^2 dp \frac{V_{kp}^{(ij)} K_{pk}^{(j)} + K_{kp}^{(i)} V_{pk}^{(ij)}}{k^2 - p^2} + \frac{4m^2}{\pi^2} \int p'^2 dp' \int p^2 dp \frac{K_{kp'}^{(i)} V_{p'p}^{(ij)} K_{pk}^{(j)}}{(k^2 - p'^2)(k^2 - p^2)}$$

3) compute the inverse matrix $(\Delta U)_{ij}^{-1}$

4) the on-shell K-matrix for $\hat{H}(\vec{C})$ is approximated as $\boxed{K_{kk} \simeq \sum_i c_i K_{kk}^{(i)}}$ with the coefficients

$$c_i = -\sum_j (\Delta U)_{ij}^{-1} \Big(K_{kk}^{(j)} + \lambda \Big), \quad \text{with} \quad \lambda = -\frac{\sum_{ij} (\Delta U)_{ji}^{-1} K_{kk}^{(i)} + 1}{\sum_{ij} (\Delta U)_{ji}^{-1}}$$

Eigenvector continuation

Example: the N4LO+ potential in the $^1S_0$ partial wave with $\overrightarrow{C} = (\tilde{C}_{1S0}, C_{1S0}, D_{1S0})$:

$$V_{p'p} \;=\; V^{1\pi}_{p'p} + V^{2\pi}_{p'p} + \underbrace{\left[\tilde{C}_{1S0} + C_{1S0}(p'^2 + p^2) + D_{1S0}\, p'^2 p^2\right] e^{-(p'^2+p^2)/\Lambda^2}}_{\text{for the actual values of } \overrightarrow{C}\text{, the short-range terms are non-perturbative}}$$

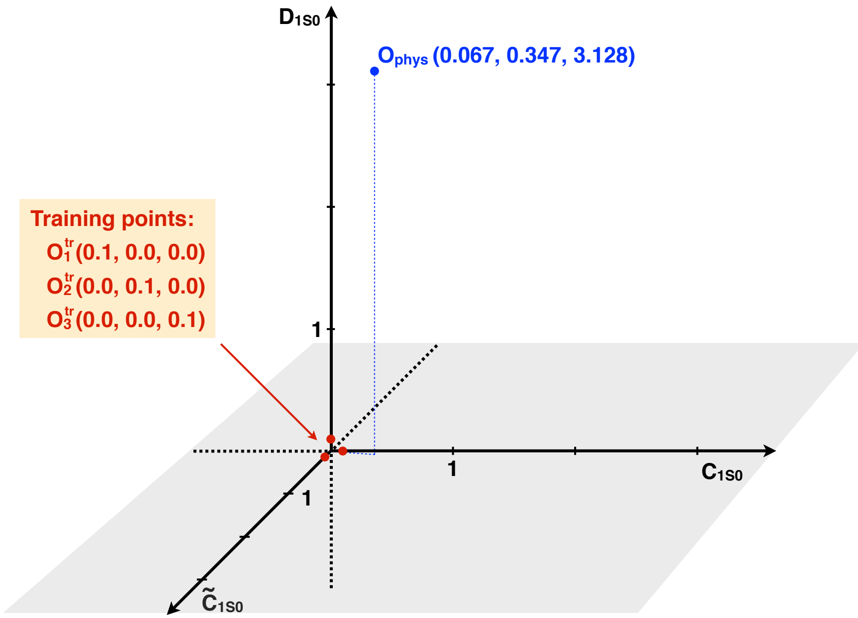

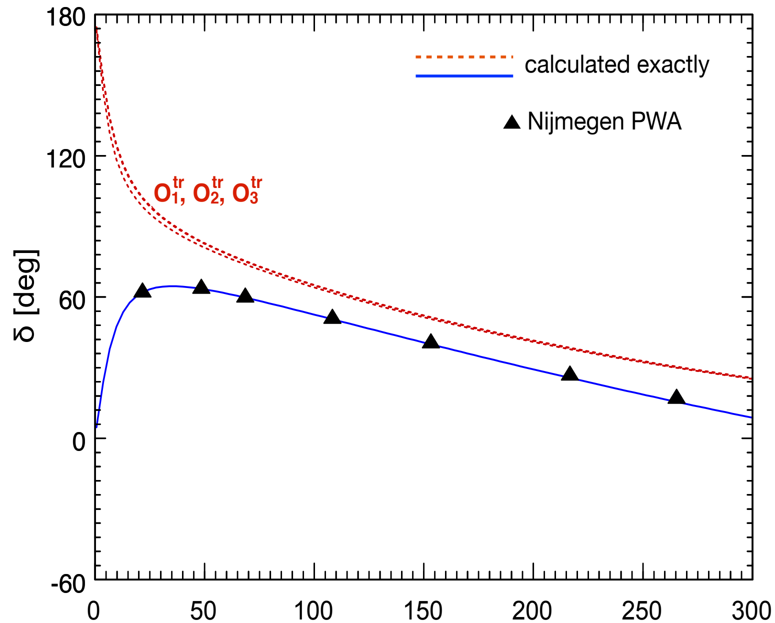

Eigenvector continuation

Example: the N⁴LO⁺ potential in the ${}^1S_0$ partial wave with $\overrightarrow{C} = (\tilde{C}_{1S0}, C_{1S0}, D_{1S0})$:

$$V_{p'p} \;=\; V^{1\pi}_{p'p} + V^{2\pi}_{p'p} + \underbrace{\left[\tilde{C}_{1S0} + C_{1S0}(p'^2 + p^2) + D_{1S0}\, p'^2 p^2\right] e^{-(p'^2+p^2)/\Lambda^2}}_{\text{for the actual values of } \overrightarrow{C}\text{, the short-range terms are non-perturbative}}$$

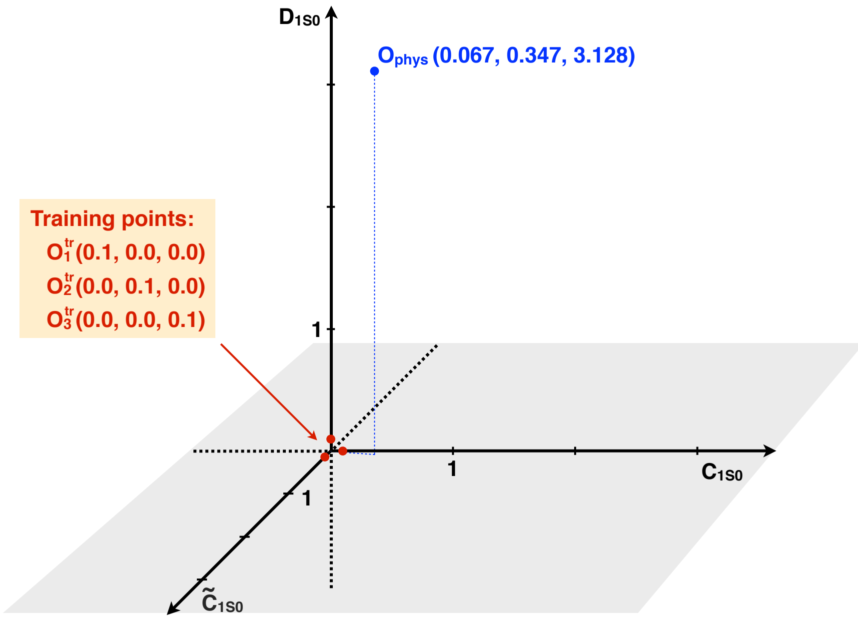

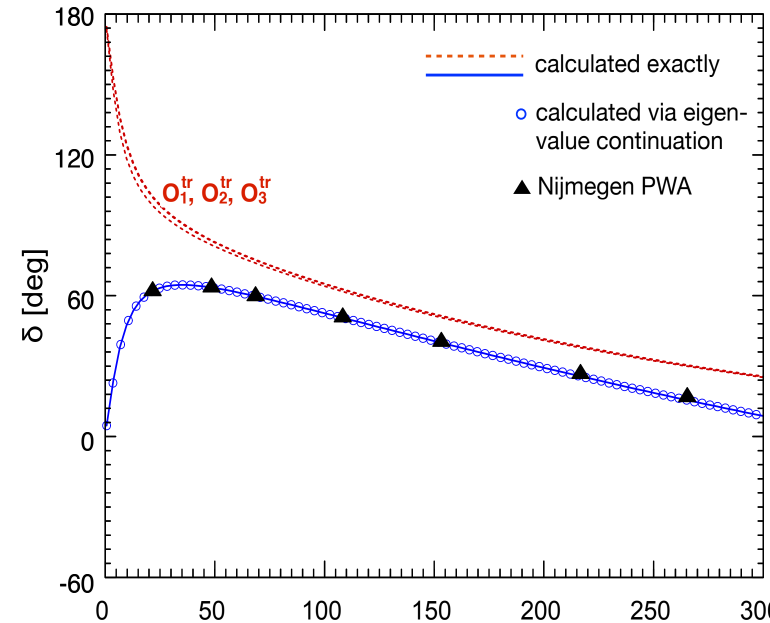

Eigenvector continuation

Example: the N⁴LO⁺ potential in the $^1S_0$ partial wave with $\vec{C} = (\tilde{C}_{1S0}, C_{1S0}, D_{1S0})$:

$$V_{p'p} = V^{1\pi}_{p'p} + V^{2\pi}_{p'p} + \underbrace{\left[\tilde{C}_{1S0} + C_{1S0}(p'^2 + p^2) + D_{1S0}\, p'^2 p^2\right] e^{-(p'^2+p^2)/\Lambda^2}}_{\text{for the actual values of } \vec{C}\text{, the short-range terms are non-perturbative}}$$

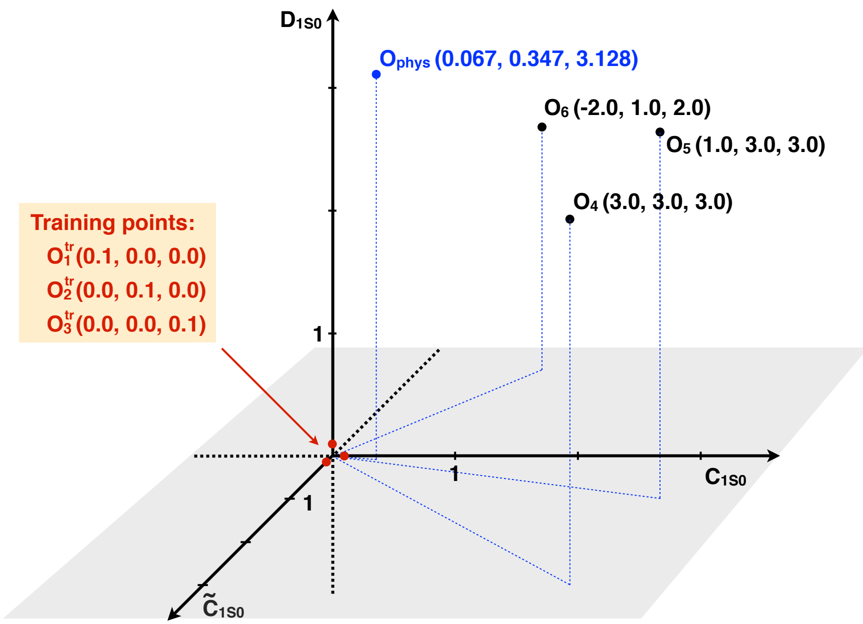

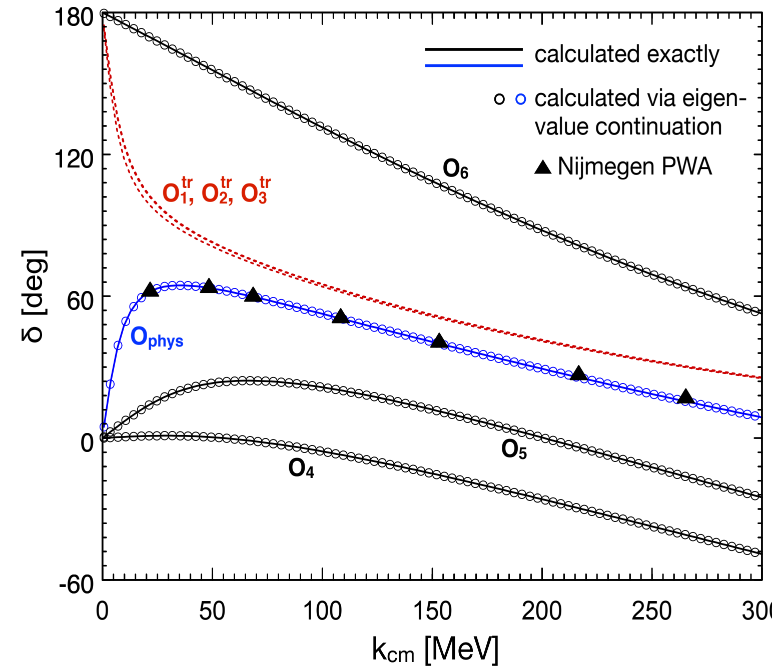

- Using just 3 training states in a tiny (perturbative) neighborhood of $\vec{C} = 0$ allows for very precise reproduction of $\delta(k)$ for all considered $\vec{C}$ and energies!
- Application to 3N scattering in progress

Summary and outlook

The 2N sector

- statistically perfect description of NN scattering data at N^4LO^+
- precision calculations of the deuteron form factors:
  - — determined $r_{\rm str}$ (0.1% accuracy) and Q_d (1.4% accuracy)
  - — combined with isotope-shift data, extracted the neutron radius

Heavier systems

- The main obstacle towards precision calculations is the uncertainty in the 3N force
- Based on the experience in the 2N system, a precise description of Nd scattering data will likely require going to N^4LO
- Major challenges:
  - — derivation of consistently regularized 3NF: Gradient flow method [Krebs, EE, in progress]
  - — determination of LECs: Eigenvector continuation [application to 3N scattering in progress]

    Also promising results using emulators based on perturbation theory [Witala et al. '21]
- More precision data for Nd elastic scattering [New exp. at RIKEN RIBF by Kimiko Sekiguchi et al.]